UNIVERSIDADE FEDERAL DE SÃO CARLOS - UFSCar
CENTER OF EXACT SCIENCES AND TECHNOLOGY - CCET
DEPARTMENT OF MECHANICAL ENGINEERING - DEMec

Pedro de Campos Muradas Cerântola

DYNAMIC CHARACTERIZATION OF A STRING MUSICAL INSTRUMENT USING OUTPUT-ONLY MODAL ANALYSIS

São Carlos - SP
2019

Pedro de Campos Muradas Cerântola

DYNAMIC CHARACTERIZATION OF A STRING MUSICAL INSTRUMENT USING OUTPUT-ONLY MODAL ANALYSIS

Undergraduate thesis presented to the Department of Mechanical Engineering of the Federal University of São Carlos for the obtaining of the bachelor's degree in Mechanical Engineering.

Advisor: Prof. Dr. Sidney Bruce Shiki

São Carlos - SP
2019

FOLHA DE APROVAÇÃO DE TRABALHO DE CONCLUSÃO DE CURSO

Resultado da avaliação da defesa pública do Trabalho de Conclusão de Curso do discente ***Pedro de Campos Muradas Cerântola***, intitulado "***Dynamic characterization of a string musical instrument using output-only modal analysis***", defendido junto ao curso de Engenharia Mecânica da Universidade Federal de São Carlos na presente data.

	Resultado:
Prof. Dr. Sidney Bruce Shiki (orientador) DEMec / UFSCar	Aprovado
Prof. Dr. Leopoldo Pisanelli Rodrigues de Oliveira Dep. de Eng. Mecânica / EESC /USP	Aprovado
Prof. Dr. Mariano Eduardo Moreno DEMec / UFSCar	Aprovado

São Carlos, 20 de dezembro de 2019

Dedico este trabalho a todos os brasileiros e brasileiras que lutam pela educação pública, gratuita e de qualidade.

Agradecimentos

Agradeço primeiramente à minha família, por toda a formação, o amor e apoio irrestritos em minha caminhada. Vó Rose, Mãe Carmen, Pai Saulo, Natália, Marília, Paula, Brasa, Dani e Maria Clara: eu amo vocês com todo o meu coração.

Aos amigos da República Boi Soberano, pelos anos maravilhosos de convivência, diversão e aprendizado.

Aos velhos amigos amados Hugo, Badu, Mary, Julia e Bel. Saudades sempre!

Aos militantes do Movimento Estudantil de São Carlos, que tantas vezes me lembraram pelo que lutar.

Aos caros amigos do Afronte! São Carlos, que me ensinaram e ensinam que lutar com quem se gosta e admira é imprescindível e tão importante quanto a própria luta. É guerra!

Aos amigos amados Mama, Gandia e Fofinho, por basicamente toda a graduação.

A todos que moraram comigo durante a graduação e que me aguentaram com louvor em partes diferentes e difíceis da minha vida.

A todos os professores de verdade com quem tive o prazer de aprender e conviver.

Aos técnicos e demais funcionários da UFSCar, pessoas de quem o trabalho árduo simplesmente possibilitou minha formatura.

Ao meu orientador Prof. Bruce, por toda a paciência e disposição de sempre em me ajudar.

Aos companheiros das 15 bandas de brincadeira totalmente provisórias e totalmente excelentes que participei em São Carlos.

À minha segunda família, que me adotou desde o fim de 2015. D. Isabelle, Sr. Paulo, Brunno, Fer, Dani e Piles, vocês estão no meu coração e têm toda minha gratidão!

À minha maior companheira de vida, namorada, amiga e professora. Loira Elisa, sem você eu não chegaria nem perto de chegar aqui, na faculdade e na vida. Te amo demais e dá pra escrever um TCC sobre o quanto eu te admiro e agradeço.

Obrigado!

"Ninguém liberta ninguém, ninguém se liberta sozinho: os homens se libertam em comunhão."

Paulo Freire

Resumo

Embora a guitarra elétrica venha sendo cada vez mais um objeto de investigação pela academia, faltam ainda conclusões contundentes a respeito de suas características dinâmicas. Para oferecer uma contribuição neste panorama, uma análise modal foi realizada tendo uma viga e uma guitarra Squier by Fender Stratocaster 50^{th} Anniversary como objetos. Juntamente com testes de bancada experimentais, estratégias de cálculo analítico e modelagem foram aplicadas à viga de aço AISI 1020, enquanto o instrumento teve sua dinâmica descrita apenas com o auxílio de dados de entrada experimentais. Para os testes, impactos de força desconhecida foram utilizados em dois locais de ambos os objetos, que foram instrumentados com quatro acelerômetros ADXL 335, todos conectados a um chassi National Instruments cDAQ-9178 equipado com um módulo medidor de tensão NI-9201. Uma placa de prototipagem Arduino UNO foi utilizada como fonte de tensão elétrica para os sensores. Após o processamento dos dados via MATLAB, as frequências naturais de 7,34, 65,43 e 107,35 Hz, respectivamente para o 1º, 3º e 4º modos de vibração da viga e 56,08, 140,65, 185,50 e 210,90 Hz para o 1º, 2º, 3º e 4º modos da guitarra foram obtidas. Um algoritmo de análise modal baseada apenas na resposta (OOMA) de decomposição no domínio da frequência (FDD) foi executado para a viga e para a guitarra, resultando nas formas corretas para o 1º, 3º e 4º modos da viga e 1º, 2º e 3º modos da guitarra. Foi verificado que o posicionamento falho dos sensores e aspectos da implementação do experimento prejudicaram alguns dos resultados obtidos. Em geral, concluiu-se que a técnica de FDD deve ser aliada a outros métodos de excitação para funcionar completamente, ao passo que as frequências naturais podem ser alcançadas a partir de procedimentos mais simples.

Palavras-chave: Vibrações mecânicas. Análise modal baseada apenas na resposta. Decomposição no domínio da frequência. Guitarra elétrica.

Abstract

Although the electric guitar has been more and more an investigation object by the academy, there are still important conclusions missing regarding its dynamic characteristics. To offer a contribution over this panorama, a modal analysis was performed having a beam and a Squier by Fender Stratocaster 50^{th} Anniversary guitar as objects. Altogether with experimental bench tests, analytical and modeling strategies were employed to the AISI 1020 steel beam, while the musical instrument had its dynamics described only with the aid of empirical inputs. For the tests, impacts of unknown force were deployed on two locations of both objects, that were instrumented with four ADXL 335 accelerometers each and connected to a National Instruments cDAQ-9178 chassis equipped with a NI-9201 voltage modulus for the data acquisition. An Arduino UNO board was used as voltage source for the sensors. After data processing via MATLAB, the natural frequencies of 7.34, 65.43 and 107.35 Hz, respectively for the 1^{st}, 3^{rd} and 4^{th} vibrational modes of the beam and 56.08, 140.65, 185.50 and 210.90 Hz for the guitar's 1^{st}, 2^{nd}, 3^{rd} and 4^{th} modes were obtained. An Output-only modal analysis (OOMA) Frequency Domain Decomposition (FDD) algorithm was performed for the beam and the guitar, resulting in correct shapes for the 1^{st}, 3^{rd} and 4^{th} beam modes and the 1^{st}, 2^{nd} and 3^{rd} guitar modes. It was verified that poor sensor positioning and implementation of the experiment hindered some of the result reached. In general, it was concluded that the FDD technique must be aligned to other excitation methods in order to fully work, while natural frequencies can be accessed through simpler methods.

Keywords: Mechanical vibrations. Output-only modal analysis. Frequency domain decomposition. Electric guitar.

List of Figures

List of Tables

Contents

1 Introduction

As an introduction, a brief contextualization of guitars development history will be presented, just like explanations on how guitars relate to engineering in terms of structure. After these topics, the motivation for the investigations made is described altogether with its objectives.

1.1 Electric guitars: history and nowadays

Electric guitars have a very rich history. Since the first half of the 20th century, when this instrument was invented (HISCOCK, 1998), two brands have been on the spotlight of musicians and enthusiasts imagery when it comes to guitars: Gibson, from 1902, and Fender, which appeared in 1946 (SOUZA, 2002).

Aside that context, guitar's evolving implied, through the course of years, on a poor, scarce developing of concepts, technologies and knowledge overall applied to the guidance of constructive and innovative capabilities. The fact that Fender and Gibson are, until current days, the two most recognizable and renowned electric guitar brands is on its own a powerful statement to that affirmation. Even more, there are not many guitar models that are, in the moment, so popular that can be counted as legendary. For example, one can cite Gibson's Les Paul and SG, and Fender's Stratocaster and Telecaster, and that is how far goes the extent of the most famous of these instruments.

Between the cited famed designs, the Fender Stratocaster is considered the most popular electric guitar of all times (TRUE FIRE, 2016). Like most of the Fender models, Stratocasters' timbre tend do be more guided to high frequencies, but there is still much to be known about the dynamic characteristics that cause that. Therefore studies that carry out a science-oriented method to investigate this aspect are certainly suitable.

One of the reasons of the gap existing on the field is exactly the existing difficulties on modeling and testing these instruments in order to obtain objective descriptive parameters. However, engineering provides tools that, if correctly applied, can help on that matter.

1.2 The electric guitar as a dynamic system

According to Felicio (2010), a dynamic system is a set of components that founds itself inside a frontier and has responses that vary over time. For dynamics and vibrations, these outputs are often related to the position or the movement of the parts, instead of mechanical properties, for example. That is a positive factor for works like the present one, as it is easier to estimate and measure variables of movement than properties.

This comes especially in hand because of one straightforward reason: just as all mechanical structures, the guitars vibrate when in use. Rao (2009) defines vibration as "any movement that repeats itself after a given period of time". With the aid of accelerometers or other sensors, that concept suits guitars as one can directly measure the spacial oscillation all mechanical parts of the guitar experience when a player pokes one or more strings.

The final product of a guitar (the sound), moreover, is itself a mechanical vibration and result of air pressure oscillations. Strings behave similarly as spring-mass-damper systems when played, and their variable distance to the pickups creates a floating electromagnetic field. That variation creates an electric signal that is conducted to the amplifier, exciting its cone periodically and, finally, producing sound. This path is represented in Figure 1.

Figure 1 – Operating principle of a guitar electromagnetic pickup

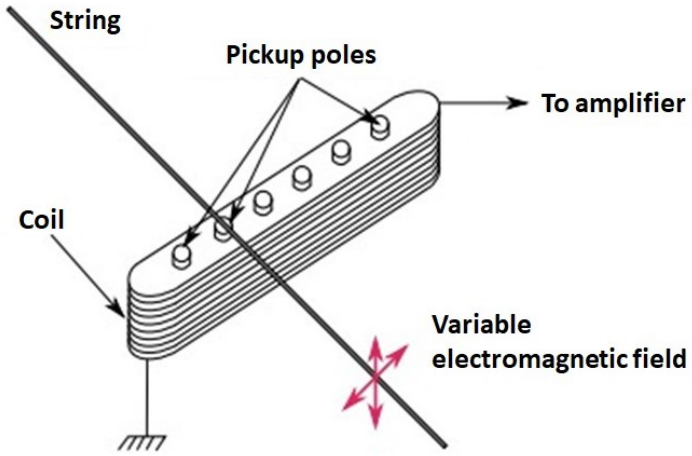

Source: adapted from Paté (2014).

Even though the structure of the guitar is not directly present on the path of sound synthesis, it does have a big influence on the observed results. This is supported by many references: Fujiso et al. (2009) found that guitars bodies' material do have an influence on listeners' perception, while Paté (2014) stated that the coupling between the strings and the body is important on how the vibration modes happen. Fleischer e Zwicker (1998) also made conclusions towards the same direction by relating the bridge stiffness to how sound energy propagates through the body of the instrument. Considering the consulted references, only Pereira et al. (2010) reached results that deviates from that, and asserted that very few of the energy of the strings is transmitted to other guitar's structures anyway, and even less energy returns to the strings, having these aspects, then, minor or no importance at all to the sound produced.

1.3 Undergraduate thesis goals and structure

Given how little dynamic aspects of guitars are investigated, the present work is proposed in order to contribute to the evolution of this area of knowledge. Following section 1.3.1 is to concisely develop and summarize that intention.

1.3.1 Objectives

The general objective of this work is to describe the dynamic properties of a Stratocaster guitar model by applying experimental and computational modal analysis methods, and so develop the mechanical engineering capabilities to deal with acoustic and music issues.

The marked main goal is directly connected to several specific points, which shall be listed hereinafter:

- To obtain the first four structural resonant frequencies of the guitar, as well as the mode shapes related to them.
- To validate an output-only modal analysis method;

1.4 Thesis structure

The work is divided in order to be the most logical and as fluid as possible. For that, subsections are used and the general argument exposition sequence is easily observed through its titles.

The text is divided henceforth in three chapters. The second one introduces a literature review over what has already been studied and developed in this thesis topics, like general mechanical vibrations theory and some other tools and methods of the same context. Authors' views and interpretations on these subjects are also considered.

In the third chapter, the methods and general aspects on which the work was developed are described. This description is supported by the contents of the previous sections.

Finally, chapter four exposes all the results achieved both by the experiments and the post-processing stages, while the conclusion and global considerations over the work here registered are presented in chapter five.

2 State of the Art

This part comprises all theoretical and developed knowledge of engineering that is related to mechanical vibrations and necessary for the full understanding of the work. Based on classical and modern literature, the text also features content on two of the pillars of the analyses made: the impact hammer testing - used to get the data - and the output-only modal analysis method of frequency domain decomposition. Finally, the specific field of electric guitars studies in vibroacoustics is addressed and reviewed.

2.1 Mechanical Vibrations theory

Often invisible to the eyes, mechanical vibrations are present in most of the movements a person comes across during a common day. People or cars passing by impact the floor, the speakers of an amplifier oscillate and transmit music, vocal cords move from side to side and have their lengths modified to make people talk and dogs bark. One way or another, all of this can be identified as vibrations.

The phenomena of mechanical vibrations is necessarily associated with a regime of oscillations that elastic materials produce to reach a stable position (NETO, 2007). Any solid body, then, has the tendency to oscillate under excitation, in order to reach a stable state. This is known as the "kinetic stability" and was first noted by Ziegler (1956).

But more than the relevance of passively using the mechanical vibrations theory to measure and observe how things oscillate in different situations, this field of knowledge is even more important as it can produce specific parameters derived by various characteristics of the bodies (such as geometry, mass and materials) that are related to the way these bodies would react to external stimuli. These are the so-called modal parameters and are usually of most relevance to the study of vibrating bodies because they can help engineers both in project and fail-preventing stages of devices or mechanisms.

One of the necessary steps to do so is to mathematically describe a physical model representing the oscillatory behavior of mechanical structures. For example, in order to obtain the response of a body in various configurations (submitted or not to external forces) models - such as the mass-spring-damper shown on Figure 2 - are developed and, in combination with their motion expressions (such as Equation 2.1 below) it is possible to describe the behavior over time or frequency of the investigated moving part.

$$m\ddot{x} + c\dot{x} + kx = f(t) \tag{2.1}$$

This model is said to have only one degree of freedom (DOF). However, the system possesses a mass (m), a damping element (c) and a stiffness element (k), associated respectively

Figure 2 – Elementary model of 1 degree of freedom

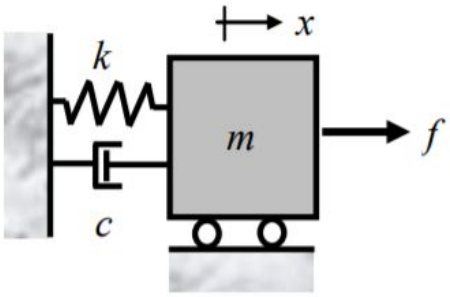

Source: adapted from Mucheroni (2012).

to the mass acceleration ($\ddot{x}$), velocity ($\dot{x}$) and displacement (x). The excitation force ($f(t)$) - an external stimuli - can be null, determining if the vibration is free or forced (MUCHERONI, 2012). Considering all elements, a second order system is formed.

With the resolution of Equation 2.1, modal parameters can be reached through the solution of an eigenvalue problem (RAO, 2009). One of the most important of these parameters is the undamped natural frequency (ω_n). According to Rao (2009), this is the value of frequency (generally given in rad/s or Hertz) in which a dynamic system tend to oscillate on free vibrations (i. e. when there is no external force acting). However, a real system has not only one natural frequency: because a body can be identified as a composition of infinite moving parts (degrees of freedom), Leckar e Sampaio (2000) stated that a n-DOF system may have n natural frequencies. The first of these values is obtained by the equation 2.2, considering the equivalent mass and siffness (k_{eq}) of the system for the 1^{st} DOF.

$$\omega_n = \sqrt{\frac{k_{eq}}{m}} \tag{2.2}$$

In realistic applications, of course, the relevant natural frequencies are of finite amount. This is due to the existence of modes of vibration (and extended not only to the frequencies themselves but also to the shapes at which their displacements occur). In terms of energy, higher modes tend to have a lower associated levels associated with, what causes modes and natural frequencies of high order to be irrelevant for the actual oscillations (JARVIS, 2017).

Aside the natural frequencies and modes shapes, another modal parameter is usually important: the normal damping associated with every mode, which is linked with the rate of amplitude diminish, is expressed as the damping ratio ζ (STEIDEL, 1989). This variable is always positive, being $\zeta = 0$ associated with an undamped system, $\zeta < 1$ an underdamped system, $\zeta = 1$ a critically damped system and $\zeta > 1$ related to an overdamped system (FELICIO, 2010). The characteristics of each kind of system with respect to the factor ζ are well-defined and can be observed in Figure 3.

Figure 3 – Normalized frequency response of a second order system for different damping factors

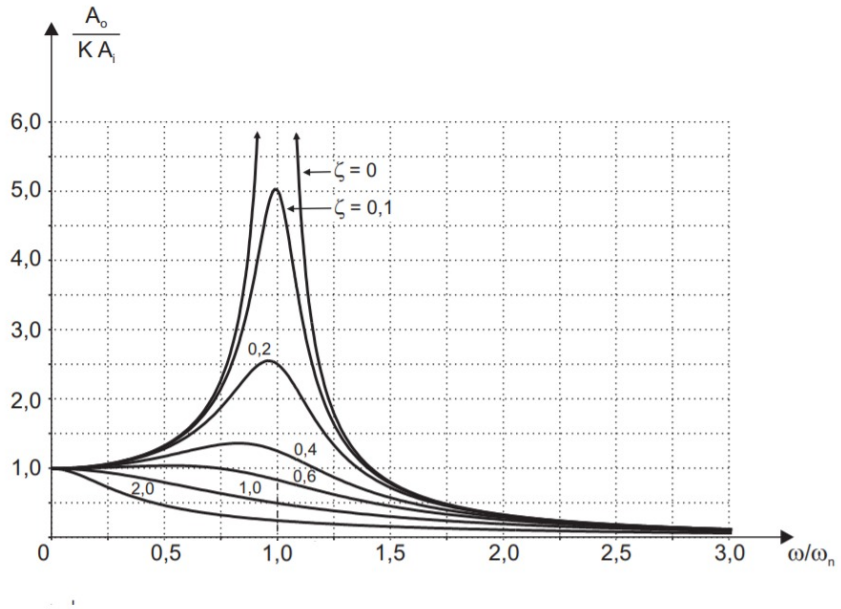

Source: adapted from Felicio (2010)

Furthermore, the values of ζ can be determined, in the case of the single DOF system, with the aid of equations 2.3 and 2.4 (RAO, 2009).

$$\zeta = \frac{c}{\bar{c}} \tag{2.3}$$

In which c is the damping coefficient of the system and $\bar{c}$ is the critical damping coefficient.

$$\bar{c} = 2\sqrt{km} \tag{2.4}$$

Having depicted the concepts of natural frequency and damping factor, one important aspect remains to characterize vibrational modes: their shape. On that matter, the beam is a commonly used representation, as this structure is abundant both for mechanical and civil engineering. Taken as a thin straight frame (with its length much bigger than its cross-section) over which only transversal forces act (TIMOSHENKO; GERE, 1983), if free constraints are considered, the first four modes of a 760 mm beam can be depicted just as in Figure 4.

Let a return be made to the eigenvalue problem mentioned. It is based on the resolution of generalization of the homogeneous part of Equation 2.1, that is, Equation 2.5 below:

$$[m]\ddot{\vec{x}} + [c]\dot{\vec{x}} + [k]\vec{x} = \vec{0} \tag{2.5}$$

Rao (2009) defines that a solution of that equation is given in the form of a set of constants multiplied by a function in time. If these constants are named X_i for each i^{th} DOF, a vector $\vec{X} = [X_1 X_2 ... X_n]^T$ can be formed for each vibration mode. This vector is called eigenvector and stores the relative position the DOFs assume on the mode taken (RAO, 2009).

Figure 4 – First four vibration mode shapes of a free-free beam

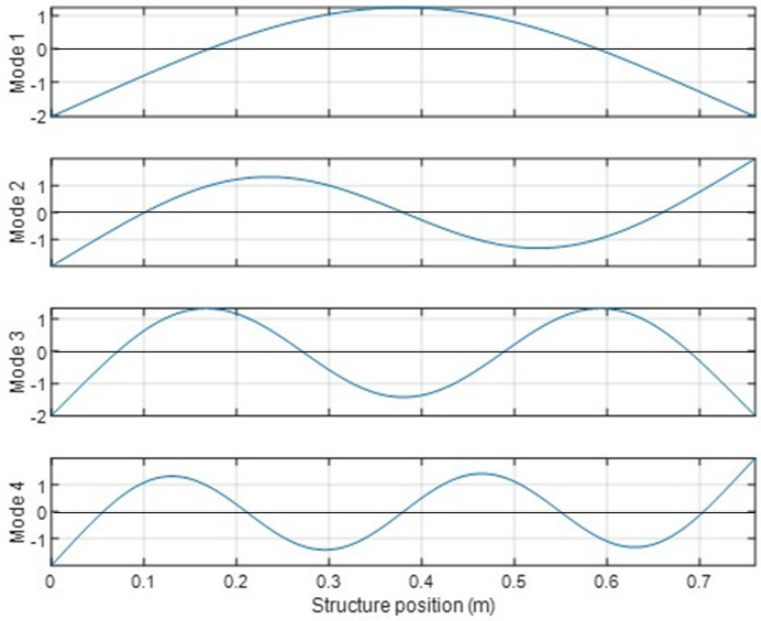

Source: Author.

Lastly, mathematical manipulations lead to Equation 2.6, that is a generalization to obtain all natural frequencies ω of the system:

$$([k] - \omega^2[m])\vec{X} = \vec{0} \tag{2.6}$$

From an experimental standpoint, however, it is not simple to obtain vibrational shapes and other modal characteristics and patterns of one given dynamic system. There are a handful of possibilities of which processes can be made to get reliable results, and these choices are related mainly to the limiting factors of the tests: whether the input is known or not, what is the nature of this input, where the sensors are attached and what is the level of noise in data are all important aspects that must be taken into account. The knowledge of modal analysis allows engineers to make smart picks on that matter, and so that is the logical next step to be talked over.

2.2 Modal analysis

In the study of dynamics, the main goal is to describe, through time, the responses of a certain system to forces and initial conditions. In modal analysis, on the other hand, the objective becomes to characterize a system through its modal parameters: their natural frequencies, damping factors and modes shapes. This is useful because these values are global (depending on the system as a whole), and in the end this kind of analysis allows for a simpler definition of the dynamic system, since less parameters are needed for a complete characterization (WAGNER, 2017).

Modal analysis is a distinct topic of many engineering fields. It is relevant, for example, to structures in civil engineering, control circuits in electric engineering and rotary shafts that transmit torque that mechanical engineers develop. Ultimately, modal analysis consists in showing variables of interest over a changing frequency - that is often treated as an input to the system.

The sequence of actions to indeed obtain modal parameters (such as the previously mentioned natural frequencies, mode shapes and damping factors) is generally not obvious. To begin with, the analysis may be divided into two categories: experimental modal analysis (EMA) and operational modal analysis (OMA) (MIELOSZYK et al., 2015). The main difference is that EMA includes both input and output data, while OMA counts only with the output info. For this reason, OMA is also called output-only modal analysis (OOMA), and that is the way it shall be treated on the present work.

The OOMA perspective is selected when it is difficult to measure the input of the modal testing. This is constantly the case in civil engineering applications, given the difficult to implement sensors efficiently in big structures under enviromental excitations (LJUNG, 1987). Into that class, a few numerical algorithms have been developed over the years: SSI-COV, SSI-DATA (in terms of subspace stochastic identification) and frequency domain decomposition (FDD, a single degree of freedom based process) are some of the numerical techniques that can be applied (CHAUHAN, 2015).

As the case of this work is of challenging evaluation of the inputs - and, moreover, the output has high level of noise - the next sections are intended to be more focused on the OOMA method of FDD. The obtaining of the output signal will be treated in more detail with a piece of text on the impact hammer test, also applied in the present case.

2.2.1 Impact hammer test

There are two main input sources for modal analyses: the shaker and the impact hammer (CRYSTAL INSTRUMENTS, 2019). The option to use one or another on modal analyses offers at the same time possibilities and limitations. The shaker, for example, excite a wide range of frequencies for sure, but generally at higher prices. Along with the need to attach the shaker to the structure tested, it might be a more efficient decision to choose for the hammer, which is a reasonably cheaper tool (REYNOLDS; PAVIC, 2000). The negative aspect of the hammer in face of the shaker is that it is usually not capable of exciting wide frequency ranges (CRYSTAL INSTRUMENTS, 2019).

In theory, considering an impulse taken over an infinitesimal time, all frequencies of a system would be excited (FELICIO, 2010). One of the ways to represent the unit impulse function is given by the Equation 2.7, that describe the known Dirac's delta function:

$$\delta(t) = lim_{\Delta t \to 0} \begin{cases} \frac{1}{\Delta t}, & t \leq \left|\frac{\Delta t}{2}\right| \\ 0, & t > \left|\frac{\Delta t}{2}\right| \end{cases} = \begin{cases} +\infty, & t = 0 \\ 0, & t \neq 0 \end{cases} \tag{2.7}$$

This means that the unit impulse function is null at any given moment, except at $t = 0$, where the function becomes infinite. The impulse is said unitary when its integral in the entire time domain equals one, as shown on Equation 2.8. The function must be multiplied by the magnitude of the impact for actual test applications.

$$\int_{-\infty}^{+\infty} \delta(t)dt = 1 \tag{2.8}$$

The goal of the hammer impact test is to mimic the impulse entry on the system. However, in a real experimental testing it is not easy to prevent double impacts of the hammer. Aside that, as seen above the impact has a infinitesimal duration, which is impossible in reality. These limitations result in having a narrower range of frequencies excited by the impact force. To get around that problem, impact hammers with different designs are used for different purposes, being selected in terms of structure and the targeted range of frequencies. Time and frequency domain features of different hammer devices are presented in Figure 5.

Figure 5 – Frequency content of various pulses

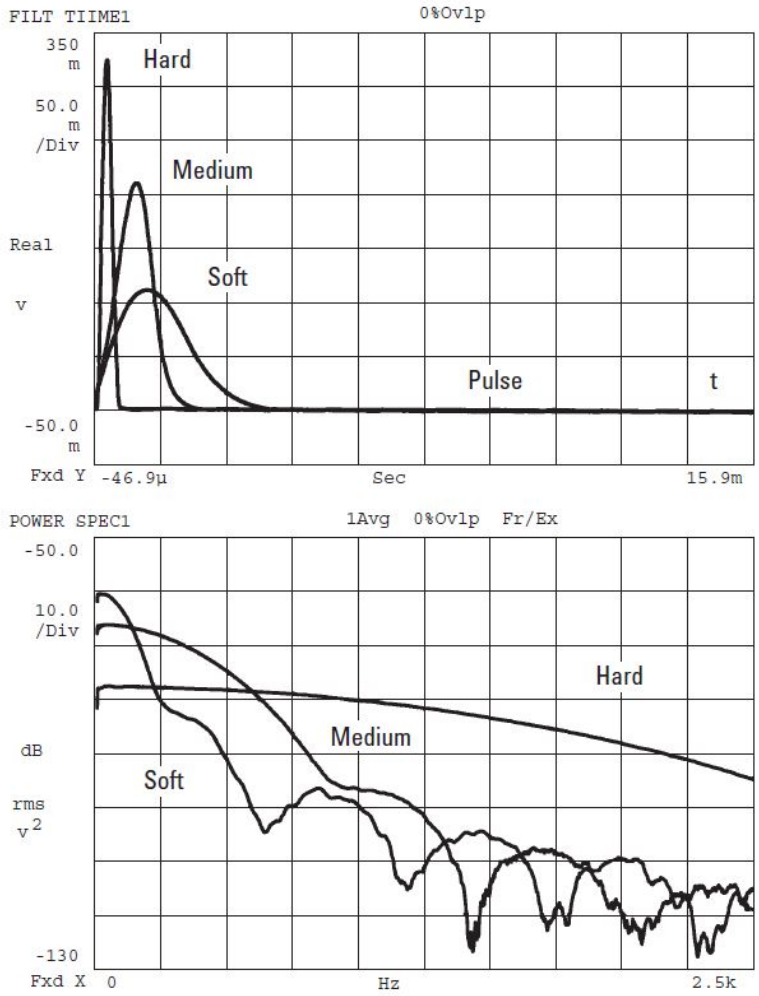

Source: adapted from Agilent Technologies (2019).

As it is easily deductible from Figure 5, the hardness of hammers' tips are the most important factor to get reliable outputs or not in a given frequency range. For example, still according to Figure 5, if one is to excite frequencies over 1 kHz, the only satisfactory hammer would be the hard one.

Another aspect that must be taken into account for the test to be well-succeeded is the expected shape of the modes of vibration. An impulse over a node of a mode, for example, would not cover that mode even with the right device. For this reason, it is generally advisable to impact the structure on multiple points.

2.2.2 An output-only method: the frequency domain decomposition

The frequency domain decomposition (FDD) is one of the newest OOMA methods developed and also one of the most practical. According to Rune et al. (2000), FDD approach allows an accurate determination of natural frequencies and mode shapes, even using signals with high levels of noise.

OOMA techniques can be arranged in two different categories: parametric (in time domain) and non-parametric (in frequency domain) (MIELOSZYK et al., 2015). Le e Tamura (2009) affirmed that non-parametric methods are better on obtaining modes shapes and natural frequencies, as parametrics, on getting damping factors. Other than more suitable to define natural frequencies and mode shapes, FDD offers also less computational cost than stochastic subspace identification (SSI) methods (RUNE et al., 2000).

Tong et al. (2005) states that the FDD technique is capable of identifying closely coupled modes by applying singular value decomposition (SVD) of multiple frequency signals. Even though the mathematical interpretation of the method is not particularly interesting for the goals of this work, it is worth saying that the main progression that technique provides is the fundamentally the division of the response in single degree of system (SDOF) systems (RUNE et al., 2000). This ends up causing complex multiple inputs and outputs (MIMO) systems to turn into various singular input and output (SISO) arrangements, facilitating the analysis.

In terms of application, it is recommended that the method should be applied under specific circumstances such as white noise excitation, small damping and orthogonal mode shapes (MIELOSZYK et al., 2015). The white noise excitation is not the case for the present work (since impacts are employed). However, due to the poor quality of measured signals in terms of noise, the other OOMA methods can be less reliable. Other than that, still according to Mieloszyk et al. (2015) the results should be trustworthy even if the white noise suggestion is not followed. As for the instrumentation steps, Section 3 will lay over this topic.

2.3 Vibroacoustics on guitars

Although most scientists are not mainly occupied with studies of vibroacoustics specifically on guitars or other musical instruments, the field has some developing and well-known

reference authors. Multiple are the views and approaches of these productions. Wallmark et al. (2018) conducted experiments to evaluate timbre perception of various instruments and at the same time correlate the data with neural activity of the subjects; Fujiso et al. (2009) performed a complete modal analysis of guitars with the same geometry and construction constrains, but diverse materials to estimate how the change on this feature affects sound; Fleischer e Zwicker (1998) operated tests to compare the energy different bridge systems transmit to the body of the instrument; Paté (2014) mixed pure vibroacoustics with perception and psychology to investigate solid body electric guitars; Pinto et al. (2016) correlated guitars made with traditional and Brazilian woods. A few manuals and collections on guitar design and manufacturing were also published, such as French (2009) and Koch (2001), in addition to general acoustics engineering works like Fahy (2005).

There are many more examples of recent contributions to the field, but one of them is directly applicable and, therefore, of interest to the development of this thesis. Russell e Pedersen (1999) ran an experimental modal analysis on a solid guitar with body shape (an Epiphone Coronet) similar to a Stratocaster, and obtained both the shapes and the natural frequencies of the first five structural modes of the instrument. Figure 6 allow the observation that both for the 1^{st} and 2^{nd} modes, the guitar behaves just like a free-free beam. This is important as the actual interpretation the present work offers towards the investigated guitar is of the instrument as a beam. The same cannot be said of the 3^{rd} and 4^{th} modes, as it is noticeable that components of torsion are present on these shapes. For this reason, the cited results shall be set as reference for the analysis that follow. The damped natural frequencies (f_n) are listed in Table 1. Those values also function as standpoints for the upcoming evaluations.

Figure 6 – First four mode shapes of an Epiphone Coronet guitar

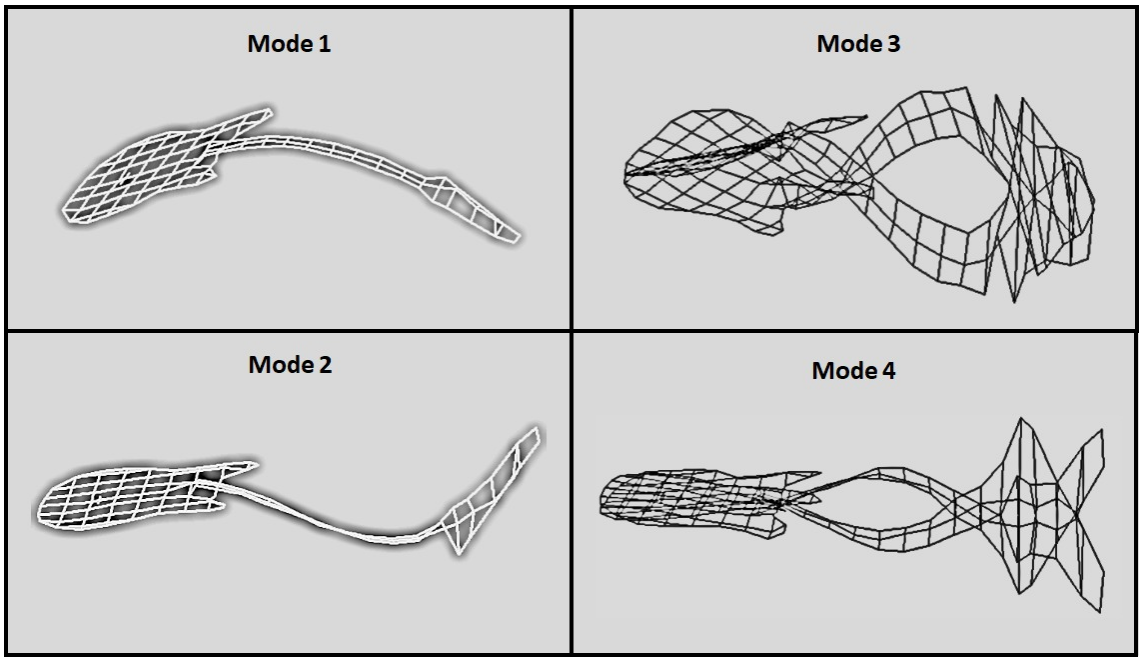

Source: adapted from Russell e Pedersen (1999).

Table 1 – First four mode natural frequencies of an Epiphone Corona guitar

Mode	f_n [Hz]
1	55.3
2	160.1
3	189.4
4	300.5

Source:Russell e Pedersen (1999).

3 Materials and methods

Three different steps were conceived for the investigation as a whole: at first, both the analytical and simulation approach of a beam were put into place. The reference for that was a piece of AISI 1020 steel with a rectangular cross section of 29.7 by 1.4 mm and 760 mm long. The properties of the cited material compose the Table 2. Both softwares MATLAB and COMSOL were used ah that initial stage, being MATLAB employed for the analytical treatment and COMSOL for the finite elements analysis (FEM) implementation.

Table 2 – Physical and geometric properties of the beam

Parameter	Value
Young's modulus [GPa]	210
Density [kg/m^3]	7870
Lenght [mm]	760
Width [mm]	29.7
Thickness [mm]	1.4

Source: MatWeb (2016).

After the modal analysis performed on finite element model of the structure, impact tests were performed with the actual beam. For that, four ADXL 335 accelerometer sensors were placed along the beam. Figures 7 and 8 show this part of the instrumentation and a graphic scheme with the distances between sensors. The accelerometers are highlighted in Figure 7 by orange circles and represented in Figure 8 by points $s1$, $s2$, $s3$ and $s4$. These sensors are capable of measuring 0.5 to 1600 Hz on axes X and Y (which was, in fact, used), and 0.5 to 550 Hz on axe Z under 1.8 to 3.6 V of input voltage (ANALOG DEVICES, 2009), which shows their suitability for the tests.

As it is seen in Figure 7, the beam is divided into 20 elements of equal length. This information is important as the tests were run using the location of elements as reference. Due to the expected mode shapes, in order to excite the first four natural frequencies of the structure, four impact tests were made: two with 10 non-measured impulses each over the elements 17 and the other two with the same amount of unknown excitations on the element 10. Figure 9 presents the location of the external forces applied on the beam. Impulses were made by hitting the structure with two different devices: a ruler and a screwdriver.

Aside from that, to assure that the constrains of free edges and transversal displacements would be predominant on the real oscillations, small pieces of string were attached to the tips and served as support for the suspended beam. In this way, not only the previously mentioned conditions were reached but also very low values of damping have been induced, maintaining, thus, the dynamical characteristics of the system. The downside of this assembly is that the wire itself induces a low pendular frequency on the oscillations that is not related to the modal frequencies of the steel beam. At the same time, thin pieces of stiff unknown metal were put to

Figure 7 – Setup for the beam's tests

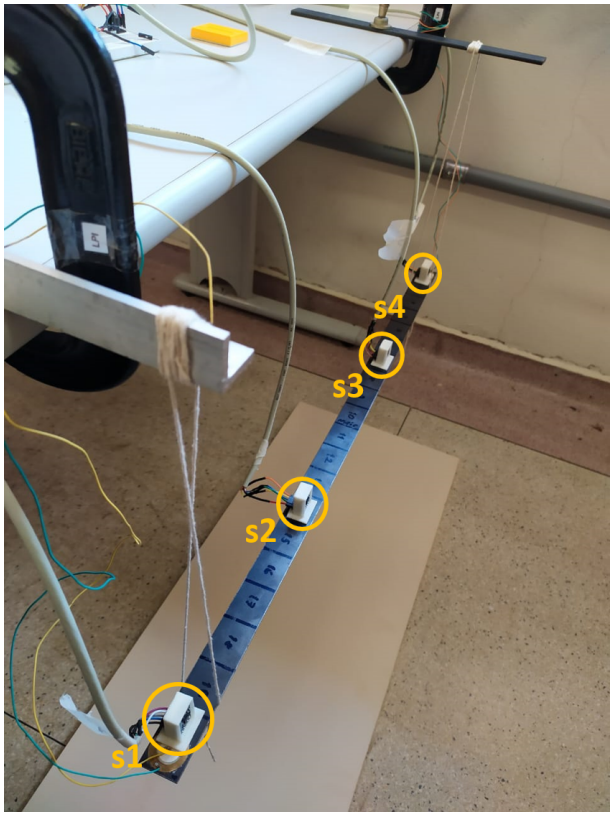

Source: Author.

Figure 8 – Sketch of the sensor's disposal on the beam

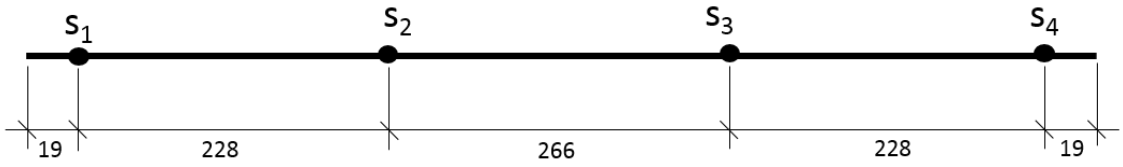

Source: Author.

Figure 9 – Sketch of the force's application disposal on the beam

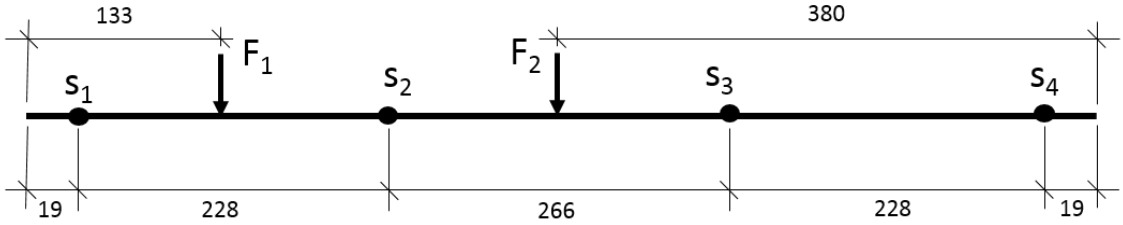

Source: Author.

use to hold the strings, which could induce different resonances with respect to the idealized system. The general aspects of the installation can also be seen in Figure 7.

For data acquisition, a straightforward setup was assembled. An Arduino UNO board served as electric voltage source for the accelerometers, and the output of the sensors was

captured with the National Instruments cDAQ-9178 chassis equipped with a NI-9201 voltage measurement modulus. As the electrical voltage and data acquisition were provided by different devices, to set one unique reference for the measurements, the ground of both the Arduino and the chassis had to be assigned as the same. That was reached by the use of a regular protoboard. An experiment routine was developed in LabView for the tests - as additional software parameters, the sampling frequency was 10000 Hz and the tests time, 10 seconds. The depicted setup can be observed in Figure 10.

Figure 10 – Setup of the instrumentation equipment

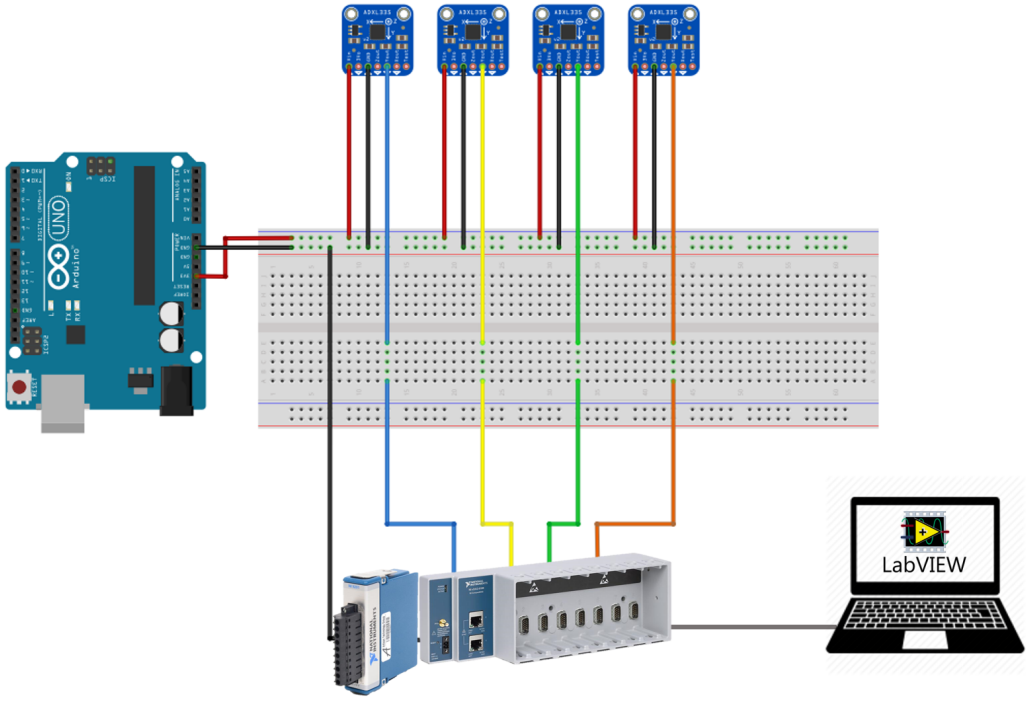

Source: Author.

The third and last step of the process included the electric guitar - more specifically, a Squier by Fender Stratocaster 50^{th} Anniversary. Experimental tests with the instrument were basically the same as with the beam: using the same fixation setup, four ADXL 335 accelerometers were distributed along the guitar (two on the body and two on the neck), as shown in Figure 11, but this time six tests were performed. The sensors fixed to the instrument are highlighted in yellow.

Each of the six tests covered six impacts, making a total of 36 impulses of unmeasured force at the two locations. The sketch in Figure 12 provides the distances between sensors (points $s1$ to $s4$) on the structure.

Just like with the beam, there were two chosen locations for the impulses: near the bridge (the metallic structure that holds the strings on the bottom part of the instrument) and by the junction of neck and body. These positions are noted on Figure 13.

For the post-processing part, the time-domain data acquired on tests (for the beam and the guitar) was considered as the input for the routines. The numerical procedures, in a first moment,

Figure 11 – Setup for the guitar's tests

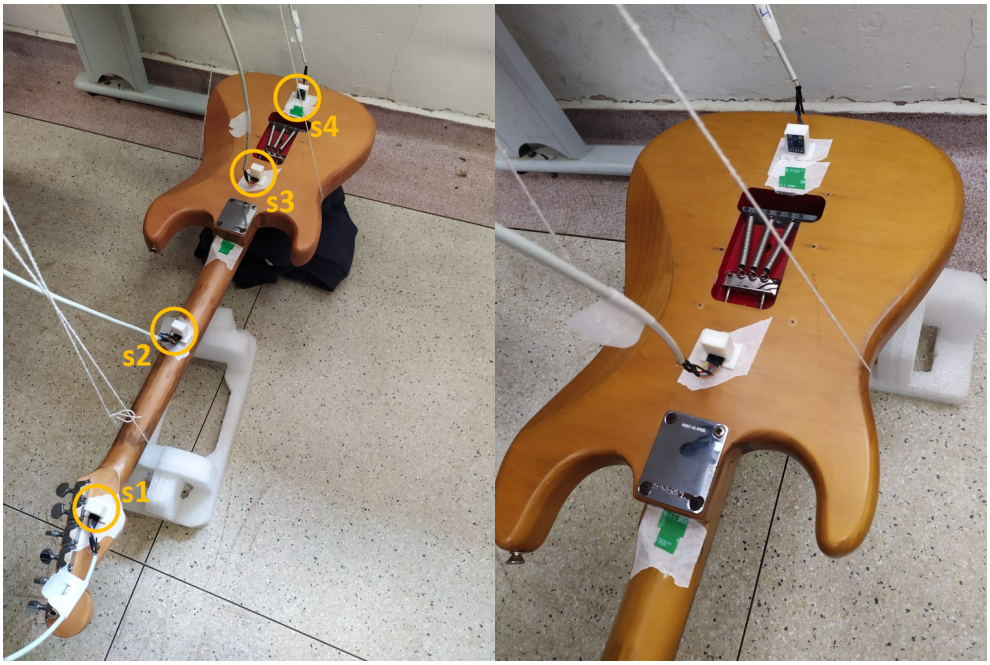

Source: Author.

Figure 12 – Sketch of the sensor's disposal on the guitar

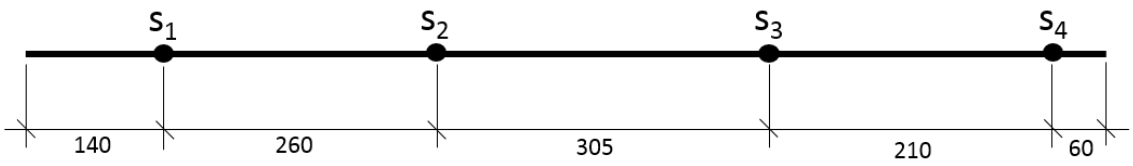

Source: Author.

Figure 13 – Sketch of the force's application on the guitar

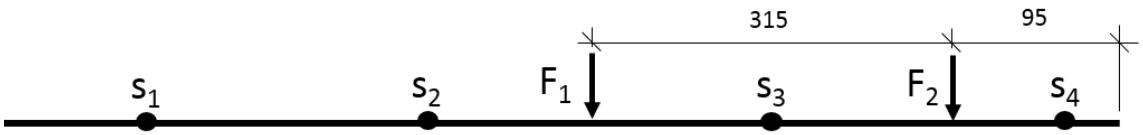

Source: Author.

were responsible for taking the fast Fourier transform of this data (fft funcion in MATLAB). After that, an algorithm of the output-only modal analysis method frequency domain decomposition was applied, in order to obtain the approximated form of the first four modes of vibration of the structures. The basic routine used is presented at the Appendix A.

4 Results and discussion

Since the procedures described in section 3 were applied almost the same both for the beam and the guitar, the present section is divided into two subsections, each one for one of these systems. The beam is treated, from now on, as a known structure used to verify and validate the analysis method to the guitar, the real intended investigation matter.

4.1 Bending vibration of a slender beam

For the beam, three main steps were enforced: the analytical calculations, and the simulation and experimental parts.

4.1.1 Analytical model

This stage consisted on the implementation of natural frequencies equations for slender beams on free vibration taken from Inman (2014) (Equations 4.1 and 4.2). According to that author, the undamped natural frequencies of slender beams can be approximated using:

$$\omega_n = {\beta_n}^2 \sqrt{\frac{EI}{\rho A}} \tag{4.1}$$

$$f_n = \frac{\omega_n}{2\pi} \tag{4.2}$$

In which ω_n is the natural frequency (in rad/s), β_n the dimensionless weighted natural frequency (both for the mode n), E the Young's modulus of the beam, I is moment of inertia, A the cross-section area of the beam, ρ the density of its material and f_n the natural frequency of the n^{th} mode in Hertz.

The values of β_n for each mode are presented in Table 3 below:

Table 3 – First four β_n of the beam - Analytical

Mode	β_n
1	6.22
2	10.33
3	14.46
4	18.60

Source: Inman (2014).

The same cited reference also defines an expression for the mode shapes of slender beams.

$$\sigma_n = \frac{cosh\beta_n l - cos\beta_n l}{sinh\beta_n l - sin\beta_n l} \tag{4.3}$$

$$-\sigma_n(sinh\beta_n x + sin\beta_n x) \tag{4.4}$$

In which σ_n is the mode shape coefficient of each mode, l is the length of the beam and x the position on the structure.

Ultimately, the natural frequencies and mode shapes obtained can be observed in Table 4 and Figure 14, respectively.

Table 4 – First four natural frequencies of the beam - Analytical

Mode	f_n [Hz]
1	12.87
2	35.48
3	69.55
4	114.97

Source:Author.

Figure 14 – Mode shapes of a slender beam - Analytical

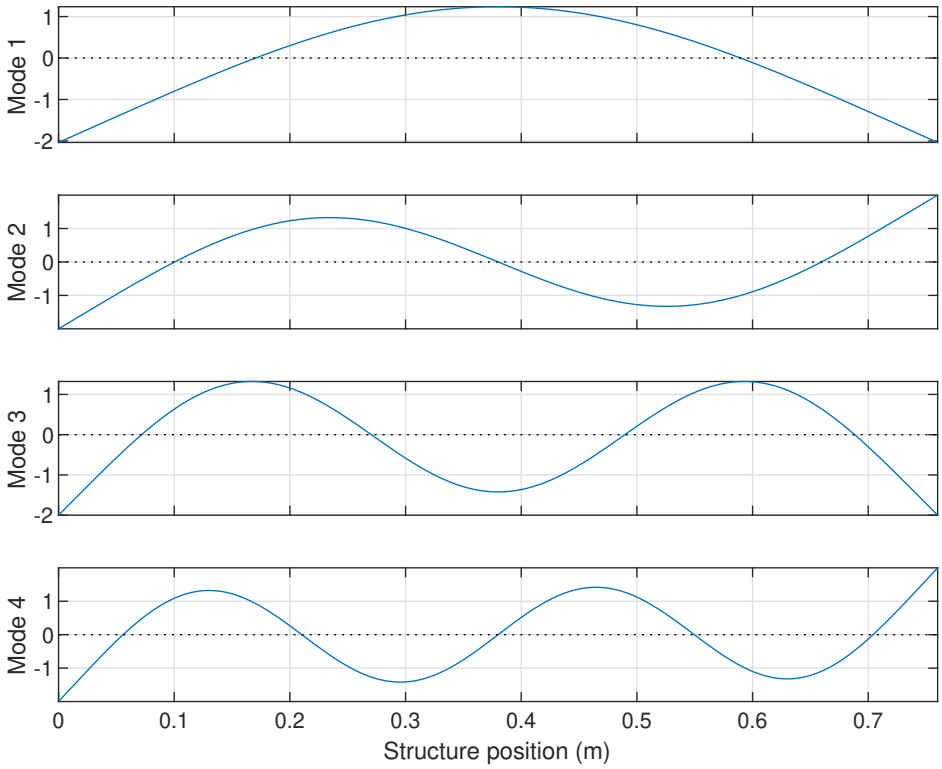

Source: Author.

4.1.2 Simulation

In COMSOL, with the beam physics and an automatic fine mesh generated by the software, both mode shapes and natural frequencies were almost identical to the analytical results. Figure 15 and Table 5 show these results. The error is obtained as the deviation between the analytical and the simulation results, being the first of these values the reference.

Figure 15 – Modes shapes - Simulation

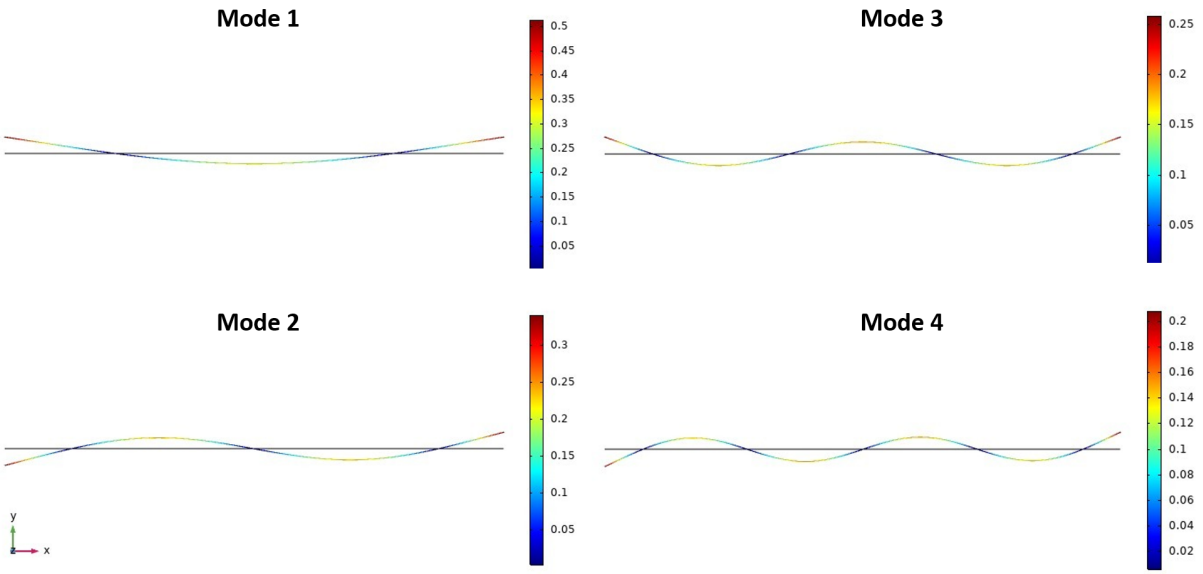

Source: Author.

Table 5 – First four natural frequencies of the beam - Analytical and simulated

Mode	f_n [Hz] (analytical)	f_n [Hz] (simulation)	Error [%]
1	12.87	12.95	0.62
2	35.48	35.69	0.59
3	69.55	69.99	0.63
4	114.97	115.78	0.71

Source:Author.

As seen in Table 5 the divergence between simulation and analytical results is minimal, what induces that the FEM model used is satisfactory.

4.1.3 Excitation on element 10

The fast Fourier transform was applied on experimental measurements of the four sensors for both test locations. The results are exposed below in form of the average Fourier transform - in other words, the simple average of the transform of all signals. Results are organized from test locations.

When the excitation force is made over element 10 (that is, the middle of the beam), modes 2 and 4 were not excited since this location is a node of these mode shapes. In this sense,

the second and fourth natural frequencies were not expected to show up in the responses to this excitation. This is visible in Figure 16. Having the analytical and simulation results, it is not expected, then, to observe frequencies around 35 and 115 Hz (roughly the 2^{nd} and 4^{th} natural frequencies presented in Table 5).

Figure 16 – Previewed modes - E.10 impact

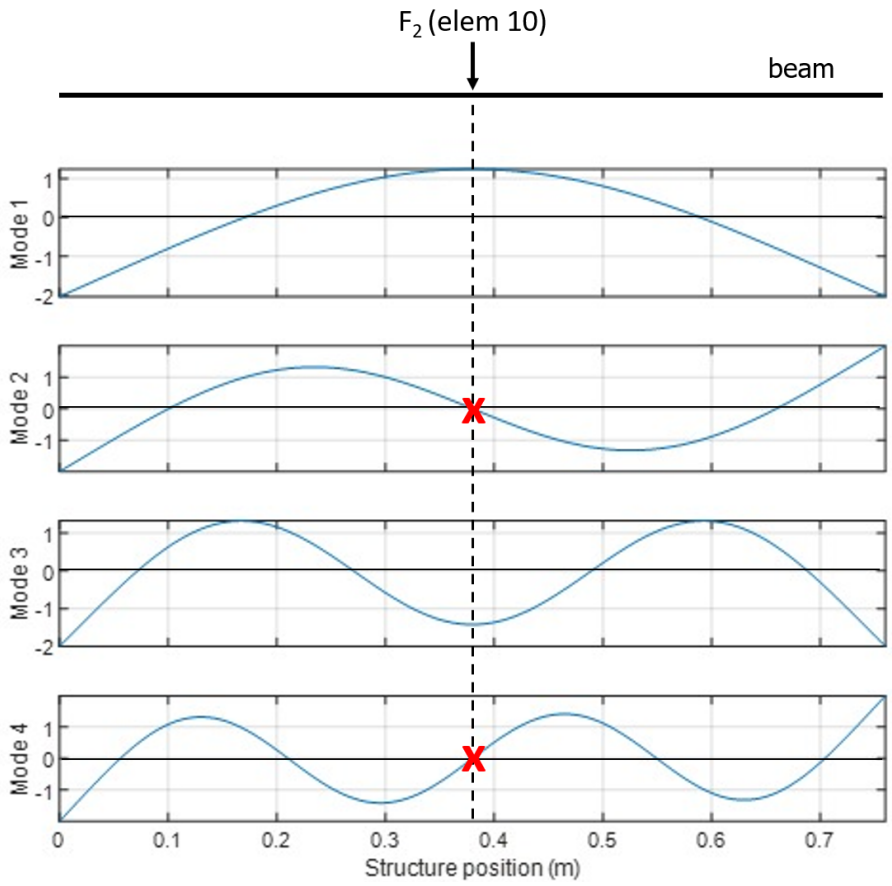

Source: Author.

However, as it is observable in Figure 17 and Table 6, probably because of minor deviations on the locations of the impulses, a frequency of approximately 107 Hz appears as a resonance. The error of the obtained values is compared to analytical results in the mentioned Table.

Table 6 – First four natural frequencies of the beam - Analytical and experimental - E.10

Mode	f_n [Hz] (analytical)	f_n [Hz] (experimental)	Error [%]
1	12.87	7.19	44.13
2	35.48	-	-
3	69.55	65.46	5.88
4	114.97	107.20	6.76

Source:Author.

Figure 17 – Superposition of average FFT's - E.10 - All sensors

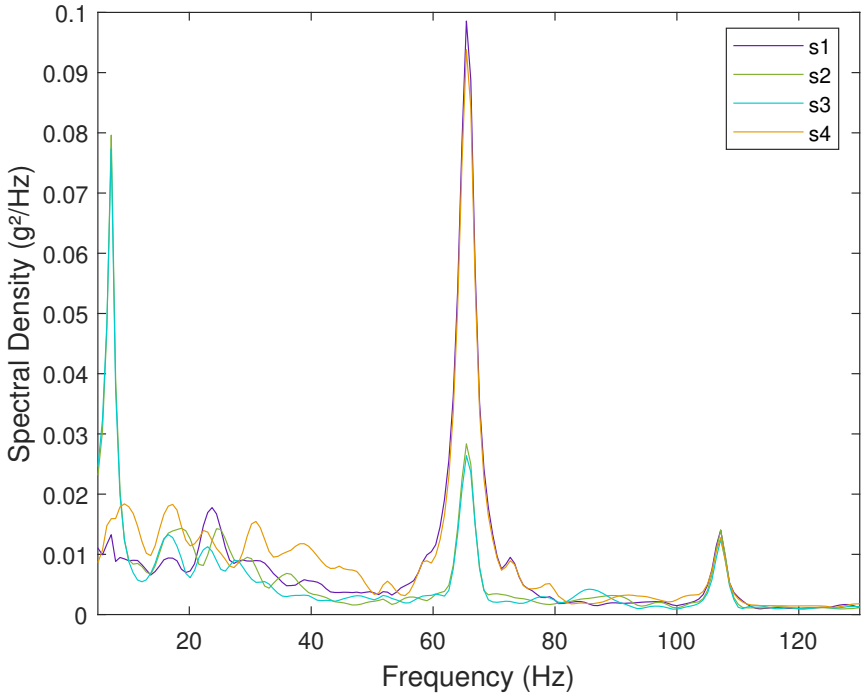

Source: Author.

As expected, the error of experimental results with the analytical method is greater than observed on previous comparison - between FEM and analytical models. This happens because the experimental data is produced, obviously, with the damping of the actual system (what was not considered in neither of the previews methods). Another reason that could explain these differences is associated to the fact that the experiment was performed under different conditions than the idealized, as the wire fixation does not correspond to free boundaries conditions.

After the obtaining of experimental natural frequencies, the FDD method was utilized on tests data. The resulting frequencies of the previous evaluation were converted to peaks selected on the FDD computation. The results can be observed in Figure 18, in which sensors positions are indicated by yellow circles (sensors 1 to 4, from the left to the right). It is prudent to conjecture, also, that the higher deviance for the 1^{st} mode could mean that this is, in fact, a rigid body resonant mode, which is not the focus of this work.

If Figure 18 is compared to Figure 4, of course, the shapes do not look the same. However, due to the fact that the experiments were made with only four sensors along the structure, it is possible to state that, exceptionally to the representation of mode 1 on Figure 18, all segments are coherent.

For the problematic mode 1, there are three options: for a first glimpse, the algorithm did not function well for sensors 1 and 4 or 2 and 3, or the own data was inconsistent. This is true because the expected final shape was of inverse values for sensor 1 with respect to 2, and 4 with respect to 3, for the same line. The erratic impulses (both on amplitude and location) probably

Figure 18 – Mode shapes - E.10 - FDD

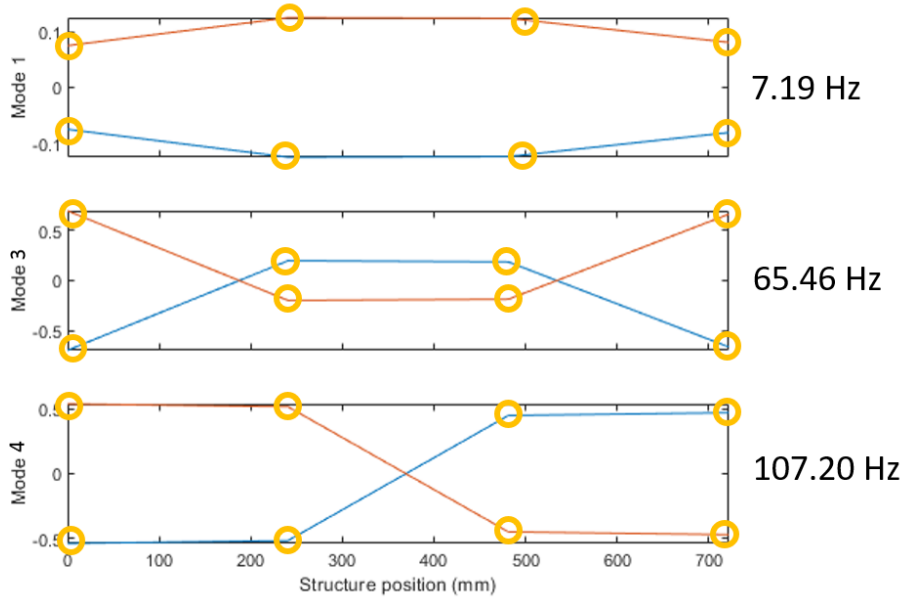

Source: Author.

affected negatively the data. A deeper inside could point, also, to a resonance induced by the setup of the experiment, or even to a rigid body mode. However, as it is shown on Figure 17, there are not observable peaks on the region of the 1^{st} resonance, what leaves no options for further analyses without more experiments.

4.1.4 Excitation on element 17

If the impact is made on element 17 of the beam, it is expected that all first four natural modes of the beam will be excited since element 17 does not coincide with a zero-displacement position on the mode shape. That statement is confirmed by Figure 19, that shows that graphically.

For the average FFT of time data, however, again the frequency that is possibly related to the second mode does not appear. This outcome is represented in Figure 20. Resonant frequencies roughly coincide with those listed in Table 6. A comparison between these values, including the error score, is presented on Table 7.

Table 7 – First four natural frequencies of the beam - Experimental - E.10 and E.17

Mode	f_n [Hz] (E.10)	f_n [Hz] (E.17)	Error [%]
1	7.19	7.48	4.03
2	-	-	-
3	65.46	65.41	0.08
4	107.20	107.50	0.28

Source:Author.

Figure 19 – Previewed modes - E.17 impact

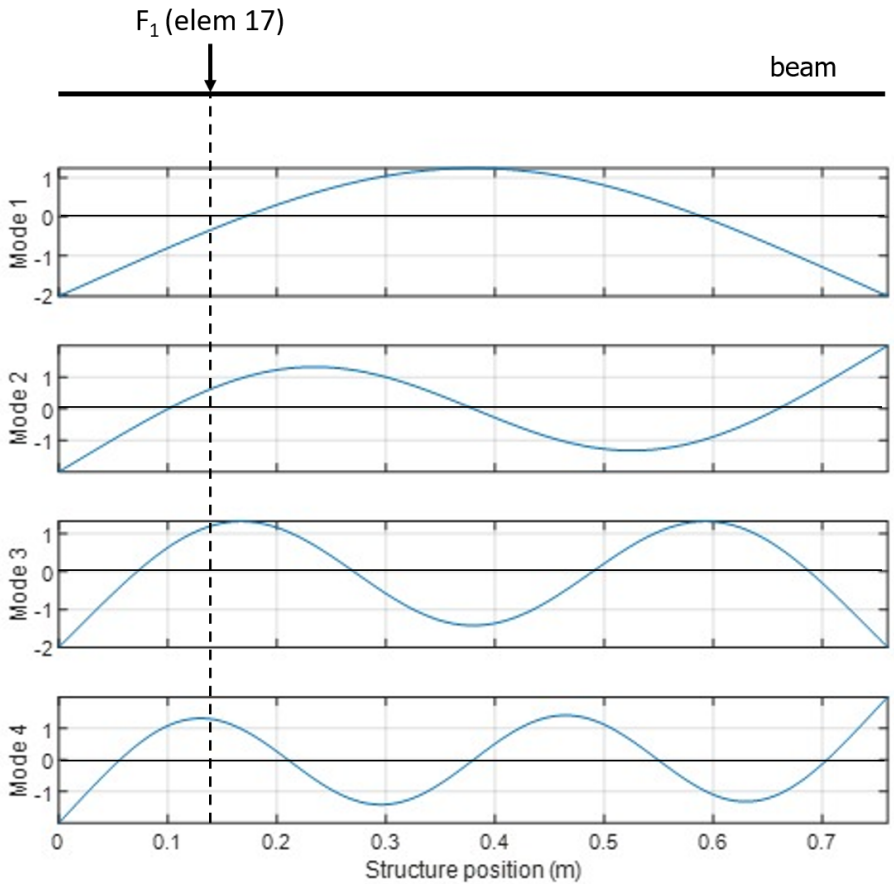

Source: Author.

Table 7 provides information that confirms the relevance of both data sets took, as the error is almost null for all resonances measured. It is safe to say, then, that these values of frequency in fact implicate resonances. Of course, the questioning about the origin of the 1^{st} of the resonances remains.

Just as done with the element 10 data, the FDD function was executed, this time for the selected frequency-data of the beam for the impacts on element 17. Figure 21 shows the shapes obtained for the modes of vibration.

Differently than with the element 10, the FDD function was able to reproduce the 1^{st}, 3^{rd} and 4^{th} mode shapes more precisely with the related input data - with the obvious detail that the output data for the sensor 3 is slightly above expected on mode 1. Those overall better results happened, possibly, because the element 17 was positioned close to the supportive cable - Figure 7 clearly shows that. For that reason, both the maximum deflection and momentum caused by impacts are smaller than in element 10, giving then much more stability to this region of the object. Being more stable, the inputs were also more reliable and directed to the center of the element, what came out as more reliable input data.

Considering all tests made with the beam, the natural frequencies and mode shapes experimentally obtained are most correctly represented on Table 7 and Figure 21, respectively.

Figure 20 – Superposition of average FFT's - E.17 - All sensors

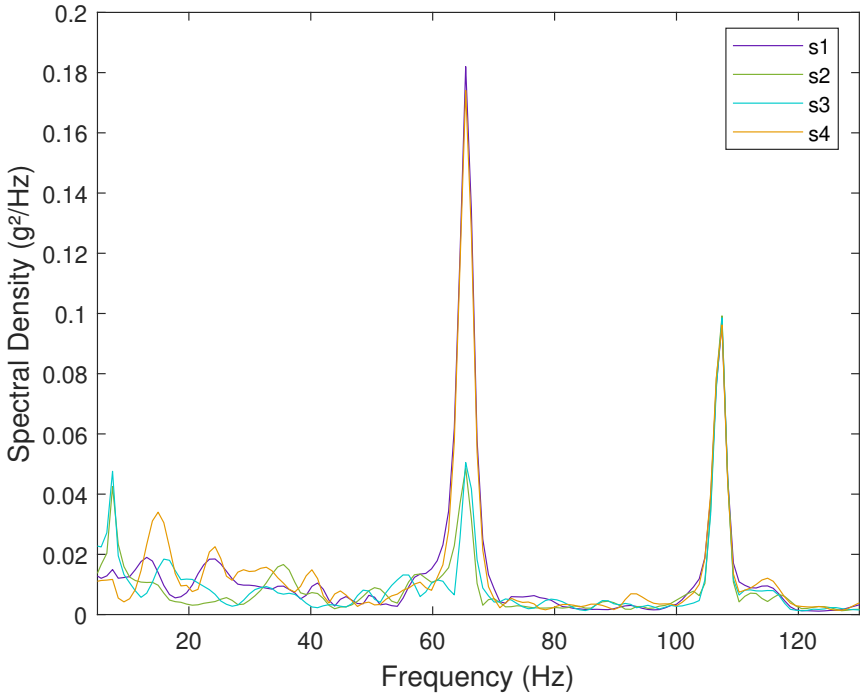

Source: Author.

Figure 21 – Mode shapes - E.17 - FDD

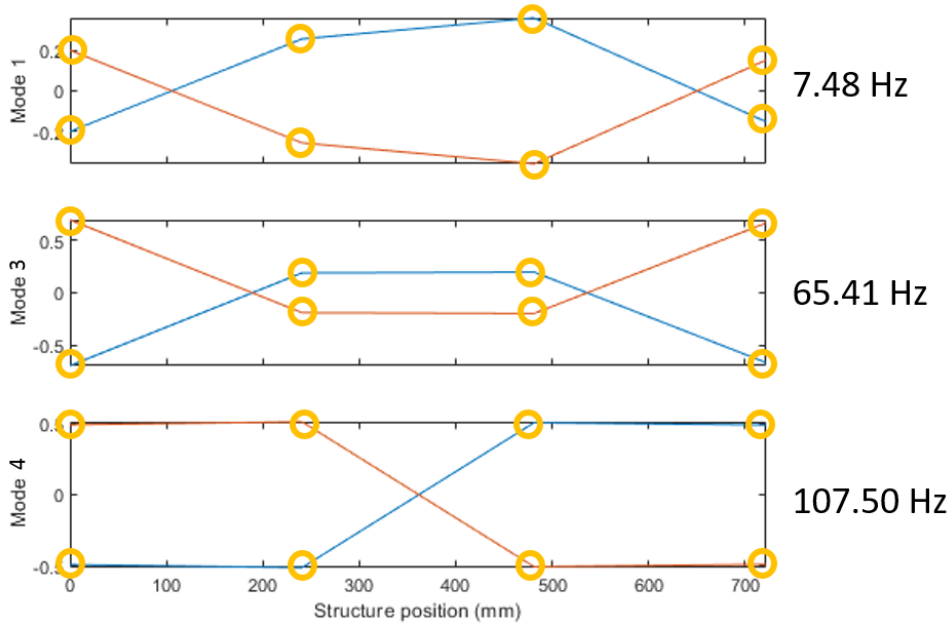

Source: Author.

4.2 Guitar

The most relevant tests for this work were the ones ran on the Stratocaster guitar. Differently than with the beam, however, no analytical or simulation results were reached as no physical model neither material's properties were available. Once again the results are divided by

the locations of the impacts made. Mode shapes are shown from the neck (left) to the body (right) of the instrument. Modes of vibration are previewed according to those of the free-free beam, but it is convenient to affirm that, because of the torsional components of guitars vibrations from its 2^{nd}, 3^{rd} and 4^{th} modes and the difference of stiffness between guitars' body and neck, the predictions are nothing but rough standpoints.

4.2.1 Excitation on body

This impact location relates to the F2 force in Figure 13. Results henceforth are presented similarly than with the beam. A careful look on Figure 22 leads to state that the impacts on the body of the guitar may be problematic on excite two of the four modes investigated: the 1^{st} (in a less precarious way) and the 2^{nd}.

Figure 22 – Previewed modes - Body impacts

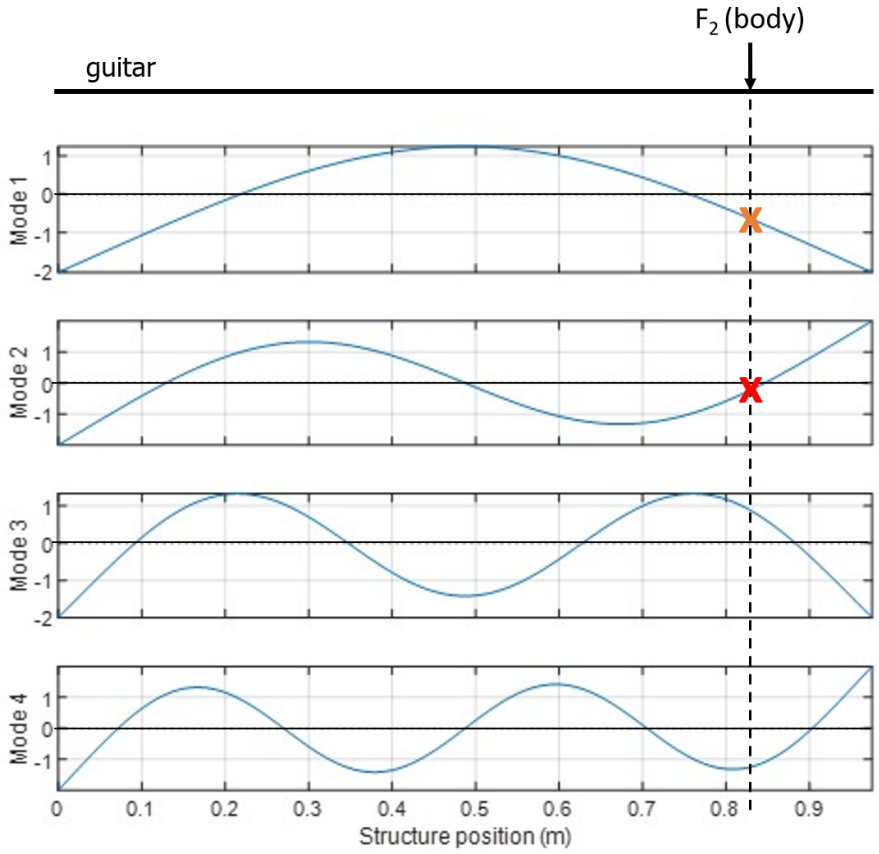

Source: Author.

This, however, was not the case specially for mode 1. Figure 23 shows that the excitation of the frequency of 56 Hz is captured by all sensors, while the 140.5 Hz mark is showed as prominent, mainly, for the sensors 3 and 4. Figure 24 offers a partial explanation for that, as the sensor 1 is located on a node of the 2nd mode.

Found resonant frequencies of Figure 23 are visually listed in Table 8.

Figure 23 – Superposition of average FFT's - Body - All sensors

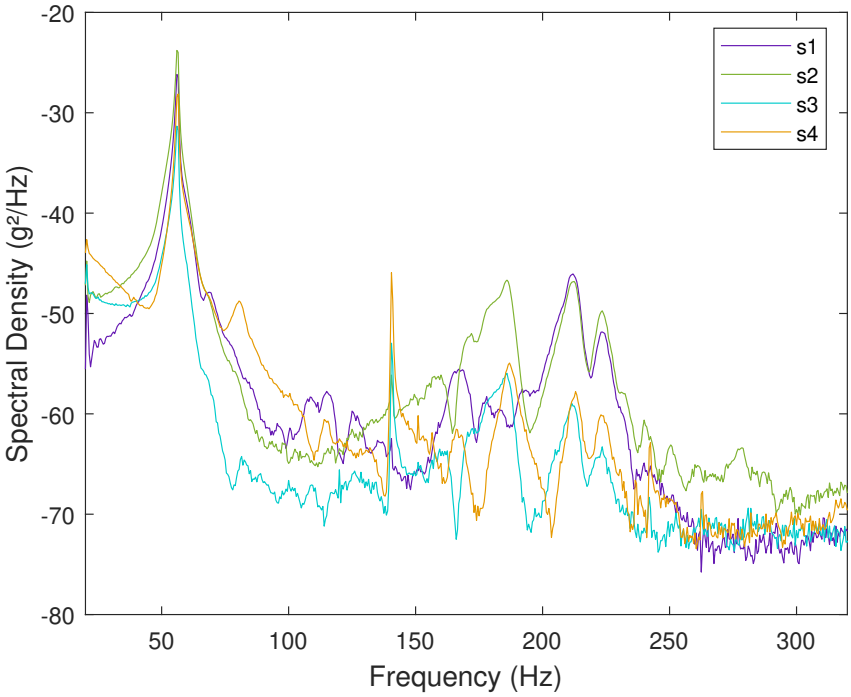

Source: Author.

Figure 24 – Previewed modes and sensors location - Guitar

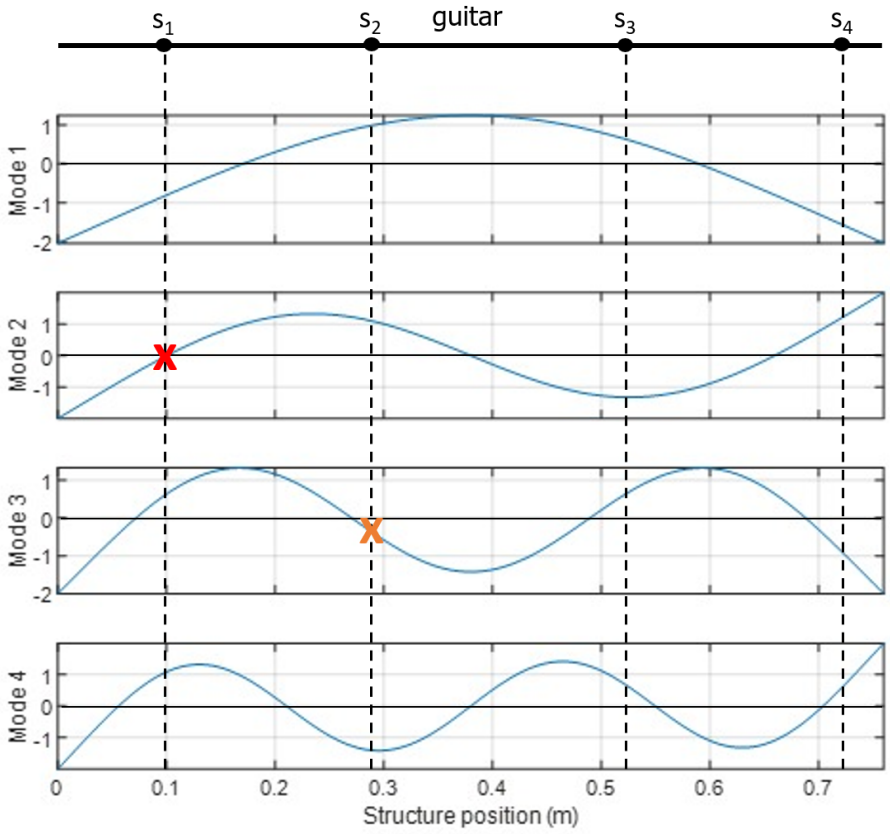

Source: Author.

Table 8 – First four natural frequencies of the guitar - Impacts on the body

Mode	f_n [Hz]
1	56.00
2	140.50
3	186.00
4	212.00

Source:Author.

Having in hands the resonance frequencies, the OOMA method of FDD is applied to the time data from the sensors with the excitation on the body of the instrument. Figure 25 shows the modal shapes obtained.

Figure 25 – Mode shapes - Body - FDD

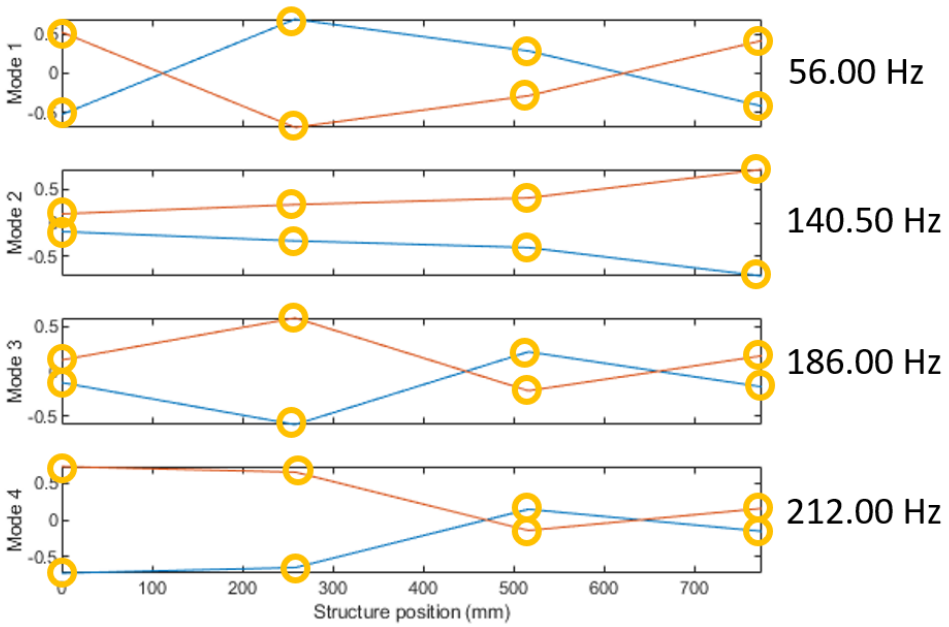

Source: Author.

With the mode shapes produced, a few observations can be made having Figure 6 as reference: the mode 1 seem to be correctly put. The different magnitudes of displacement of sensors 2 and 3 are explained both by the asymmetrical manner these sensors are disposed on the guitar and the different properties of the locations to which they were attached. Mode 3, in addition, was also satisfactorily shown, but the same cannot be said of modes 2 and 4. The fact that these modes present smaller displacement on body sensors may have affected negatively sensors data. Other aspects worth-mentioning for that go from the bad quality of the impacts on the instrument to the sources of noise inputed to the measurement. Also, it is again plausible to state that the suspended guitar is not an assembly with proper free boundary conditions.

4.2.2 Excitation on the neck

In opposition to the other excitation location, the neck of the instrument corresponds to the F1 force in Figure 13. Once again the same sequence of results presentation is granted in the following parts.

The probable nodes locations that the impacts overlay are exposed in Figure 26. As it can be seen, mode 2 should be only partially excited and could result on inferior results for the natural frequencies and shapes with the FDD application.

Figure 26 – Previewed modes - Neck impact

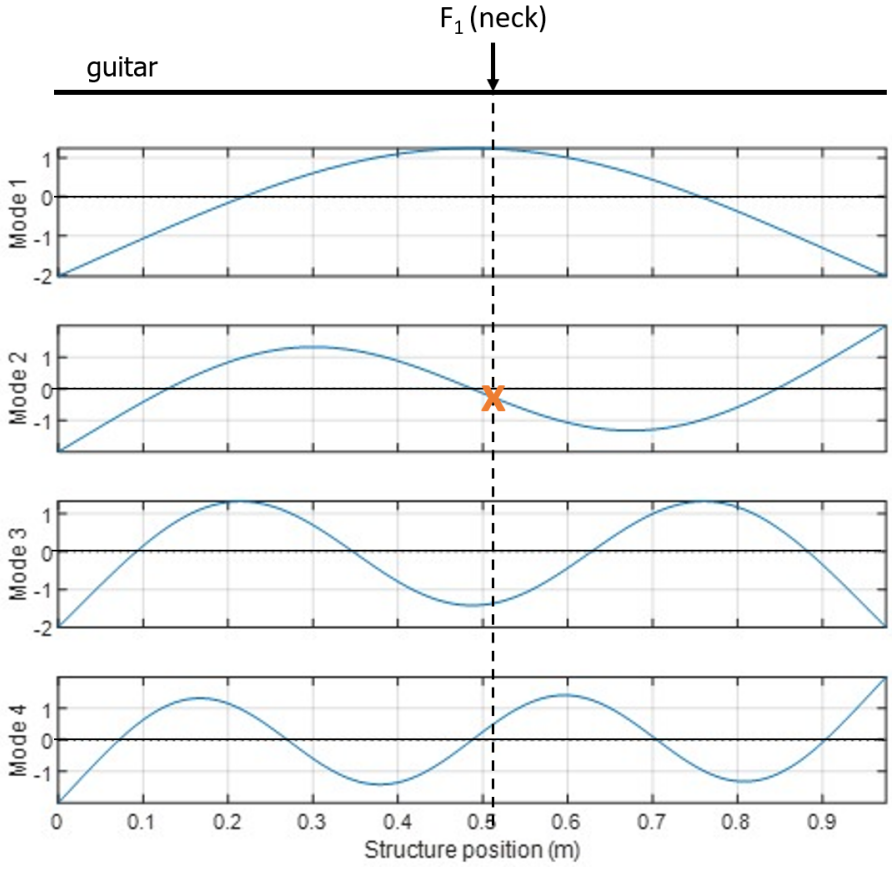

Source: Author.

This possible defect is shown in the correlate FFT image. In Figure 27 it is observable that the 2^{nd} natural frequency is minoritarily perceived, especially by sensor 3 and not recognized at all by sensor 1. That detail is noted in Figure 28.

Figure 24 provides an interpretation on why that fact occur, as the sensor 1 is positioned right at a node of the 2^{nd} mode of vibration.

Either way, all four resonant frequencies have highlighted appearances on Figure 27. The values of these modal parameters are listed in Table 9 and compared with the ones obtained by the previous test.

Finally, the FDD algorithm was performed once more, this turn with the data produced by the impulses on the neck of the instrument. Figure 29 contains the obtained mode shapes.

Figure 27 – Superposition of average FFT's - Neck - All sensors

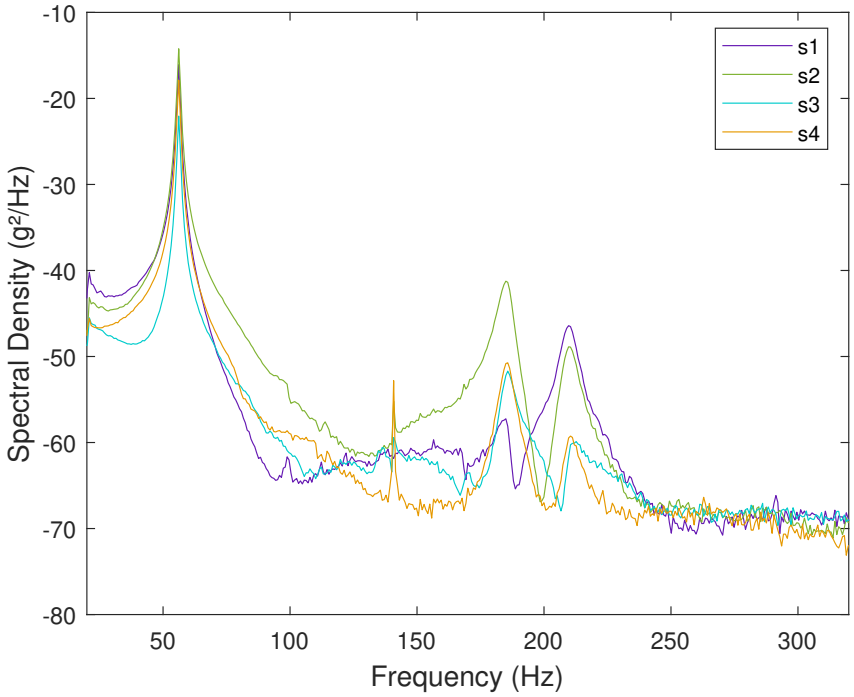

Source: Author.

Figure 28 – Superposition of average FFT's - Neck - All sensors - 2^{nd} natural frequency

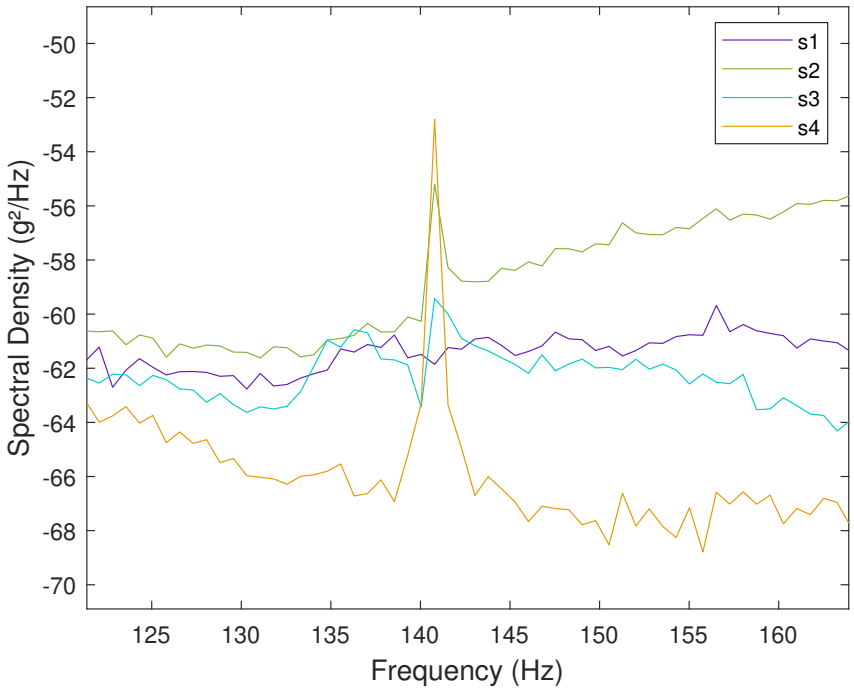

Source: Author.

Once again modes 1 and 3 are correctly produced with the FDD method. This time, distinctly than with the body Figures, mode 2 is also accomplished with relative precision. In

Table 9 – First four natural frequencies of the guitar - Body and neck

Mode	f_n [Hz] (Body)	f_n [Hz] (Neck)	Error [%]
1	56.00	56.17	0.30
2	140.50	140.80	0.21
3	186.00	185.00	0.54
4	212.00	209.70	1.09

Source:Author.

Figure 29 – Mode shapes - Neck - FDD

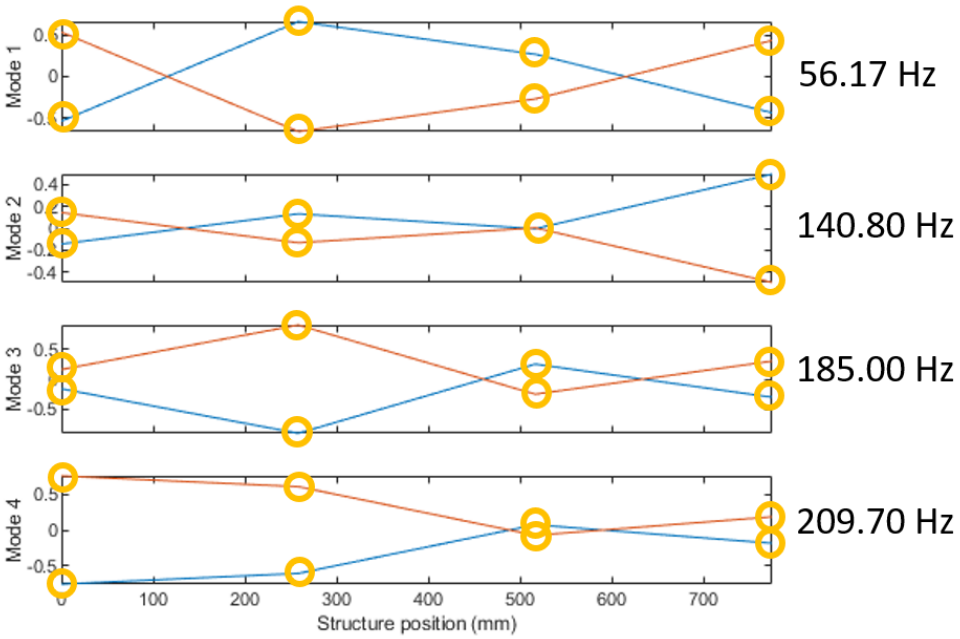

Source: Author.

that analysis, however, mode 4 is incorrect. The difference of stiffness between the body and the neck of the guitar may have contributed to these errors in general, since vibrations certainly propagates unequally through these structures. In addition, all flawed conditions discussed before continued to act.

5 Conclusions

The present work had as main objective to describe the dynamic characteristics of an electric guitar through the performance of an output-only modal analysis. To do so, tools and concepts of mechanical vibrations were put to use, such as concepts of dynamic systems under different conditions of excitation, the application of Fourier transform on time domain signals and the use of the output-only modal analysis method of frequency domain decomposition.

Having based all the actual analysis of the guitar on highly similar methods made over a known structure - an instrumented slender beam - a few considerations can be made. In the first place, it is easy to note that the analytical and simulation handling of the beam were well-implemented, given the minor error between results of both natures.

With these references in hand and the bench tests done, it was possible to numerically process experimental data and to compare it with the previous results. This was enlightening, given the fact that three of the four first modal frequencies were obtained empirically with reasonable precision. The absence of the 2^{nd} modal frequency on rendered data, however, was a strong indicator that the actual tests were not capable of offering full accurate evidences of the true nature of the objects investigated.

The fact that experiments showed to produce some unreliable data was itself important for the continuation of the analyses. With the connection of the different steps performed, the deficiency of the test was recognized to be associated with two main factors: the location of sensors and external input (the impulse forces made to excite the structure) were not optimized if the nodes of modes are to be considered and the realized suspension method was not capable of deliver real free constraints boundary conditions.

All arguments presented, it is possible to sustain that the beam formed, in general, an efficient standpoint to the analyses on the guitar dynamic characteristics. Taking that object into account, the experiments stumbled upon similar limitations. However, the substantial differences of both structures played a parallel role in that stage of the work.

For instance, the fact that the guitar is composed of two main parts (the body and the neck) with vast variation of stiffness makes sensors prove sensitive differences in terms of magnitude of the output signal. Even though the response of the sensors were normalized, to guarantee smoother results, the amplitudes kept their relative gap. This is not wrong per say, but can be misleading as the FDD method, for example, do not take these particularities into account properly.

Although these factors cannot be simply ruled out of any stage of the investigation, the modal analysis functioned perfectly well in terms of obtaining the first four modal frequencies. It is easy to attest this statement as all four frequencies appeared on the tests of both locations with great similarity.

Finally, it is prudent to declare that while the FFT function used on MATLAB worked

well with the guitar's data in general, the FDD method had several problems that have prevented totally reliable results. With exception of the 1^{st} and 3^{rd} modes for both locations and the 2^{nd} mode for the impacts on the neck of the instrument, mode shapes produced were untrustworthy. Aside the questions already brought, the fact that guitar's asymmetry deliver torsional components to the vibrations makes even more important the usage of more than four sensors to correctly detect modes shapes.

In terms of its technical intentions, the work can be considered satisfactory. The learning curve towards the possibilities and limitations of OOMA, in company with the understanding of the factors that have contributed for the results obtained, were crucial for the next steps to emerge.

5.1 Next steps

Having concluded this investigation, a few possibilities on how to evolve modal analysis methods employed arise. Two supplementary modifications could be made in order to produce enhanced results: to make impacts on more locations (a sweep with an impact hammer would fit, for example) and to use a shaker excitation in order to get around modes nodes and to guarantee the stimulation of wider ranges of frequencies via white noise. The strategy of roving sensors can also be applied, considering the context of limitations in number of available sensors.

Other possible adaptation regards the suspensions system of the guitar, as foam pieces could be used to guarantee smaller influence of induced stiffness and damping.

Aside those suggestions, a modeling component could be added on the figure of a FEM model of the guitar. This way, the existence of more solid standpoint references could assist on the evaluation of experimental designing and testing.

Bibliography

AGILENT TECHNOLOGIES. *The Fundamentals of Modal Testing*. 2019. <http: /www.modalshop.com/techlibrary>. Last access: 12/09/2019.

ANALOG DEVICES. *Accelerometer ADXL 335*. 2009. <https://www.sparkfun.com/datasheets/Components/SMD/adxl335.pdf>. Last access: 12/13/2019.

CHAUHAN, S. Parameter estimation algorithms in operational modal analysis: A review. *International Operational Modal Analysis Conference*, Gijón, Spain, n. 6, p. 1–11, 2015.

CRYSTAL INSTRUMENTS. *Modal Testing*. 2019. <https://www.crystalinstruments.com/modal-testing>. Last access: 12/09/2019.

FAHY, F. *Foundations of Engineering Acoustics*. Cornwall, UK: Elsevier Academic Press, 2005.

FELICIO, L. C. *Modelagem da Dinâmica de Sistemas e Estudo da Resposta*. São Carlos, Brazil: RiMa Editora, 2010.

FLEISCHER, H.; ZWICKER, T. Mechanical vibrations of electric guitars. *Revista Acta Acustica*, Acustica, Icking, Germany, v. 84, p. 758–765, 1998.

FRENCH, R. M. *Engineering the Guitar: Theory and Practice*. New York, USA: Springer, 2009.

FUJISO, Y.; CARROU, J. L. L.; OLLIVIER, F. Vibroacoustical study of a solid-body electric guitar. Chalmers University of Technology, Göteborg, Sweden, 2009.

HISCOCK, M. *Make Your Own Electric Guitar*. Hampshire, United Kingdom: Blandford Press, 1998.

INMAN, D. J. *Engineering Vibration*. New Jersey, USA: Pearson Education, 2014.

JARVIS, M. *Waves Normal Modes*. London, UK: Oxford University, 2017. <https: //www2.physics.ox.ac.uk/sites/default/files/2012-09-04/fullnotes2016_pdf_91657.pdf>. Last access: 12/10/2019.

KOCH, M. *Building Electric Guitars: How to Make Solid-Body, Hollow-Body and Semi-Acoustic Electric Guitars and Bass Guitars*. Gleisdorf, Austria: Martin Koch, 2001.

LE, T. H.; TAMURA, Y. Modal identification of ambient vibration structure using frequency domain decomposition and wavelet transform. *The Seventh Asia-Pacific Conference on Wind Engineering*, APCWE, Taipei, Taiwan, p. 1–8, 2009.

LECKAR, H.; SAMPAIO, R. Aspectos matemáticos de vibrações mecânicas. Rio de Janeiro, Brazil, 2000.

LJUNG, L. *System Identifications: Theory for the User*. New Jersey, USA: PTR Prentice Hall, 1987.

MATWEB. *Source for Materials Information*. 2016. <http://www.matweb.com/index.aspx>. Last access: 12/10/2019.

MIELOSZYK, M.; OPOKA, S.; OSTACHOWICZ, W. Frequency domain decomposition performed on the strain data obtained from the aluminium model of an offshore support structure. *Journal of Physics* — Conference Series, Warsaw, Poland, n. 628, p. 1–7, 2015.

MUCHERONI, M. F. *Dinâmica de Sistemas Discretizados - Vibrações Mecânicas*. São Carlos, Brazil: [s.n.], 2012.

NETO, A. P. R. *Vibrações Mecânica*. Rio de Janeiro, Brazil: E-papers Serviçoes Editoriais LTDA., 2007.

PATÉ, A. Lutherie de la guitare électrique solid body : aspects mécaniques et perceptifs. Université Pierre et Marie Curie, Paris, France, 2014.

PEREIRA, R. M.; JUNIOR, A. L.; FREITAS, T. C. Sobre o acoplamento corda-corpo em guitarras elétricas e sua relação com o timbre do instrumento. Physicae, Curitiba, Brazil, 2010.

PINTO, T. H. L.; SILVA, O. C. D.; VANZELA, A. Processamento de sinais aplicado À anÁlise comparativa do timbre de instrumentos produzidos com madeiras nacionais e tradicionais. *Simpósio de Mecânica Computacional*, Diamantina, Brazil, XII, 2016.

RAO, S. *Vibrações Mecânica*. São Paulo, Brazil: Pearson Education do Brasil, 2009.

REYNOLDS, P.; PAVIC, A. Impulse hammer versus shaker excitation for the modal testing of building floors. *Experimental Techniques*, Springer, Zürich, Switzerland, p. 39–44, 2000.

RUNE, B.; ZHANG, L.; ANDERSEN, P. Modal identification from ambient responses using frequency domain decomposition. *International Modal Analysis Conference - IMAC*, San Antonio, USA, n. 18, p. 624–630, 2000.

RUSSELL, D.; PEDERSEN, P. *Modal Analysis of an Electric Guitar*. Flint, USA: Kettering University, 1999. <https://www.acs.psu.edu/drussell/guitars/electric.html>. Last access: 12/10/2019.

SOUZA, N. Guitarra elétrica: um ícone na cultura pop do século xx. *Revista Vernáculo* — Revista do Departamento de História da UFPR, Curitiba, Brazil, n. 5, p. 33–45, 2002. ISSN 2317-4021.

STEIDEL, R. F. J. *An Introduction to Mechanical Vibrations*. New Jersey, USA: John Wiley and Sons, 1989.

TIMOSHENKO, S. P.; GERE, J. E. *Mecânica dos Sólidos*. Rio de Janeiro, Brazil: Livros Técnicos e Científicos S.A., 1983.

TONG, W.; LINGMI, Z.; YUKIO, T. An operational modal analysis method in frequency and spatial domain. *EARTHWUAKE ENGINEERING AND ENGINEERING VIBRATION*, Beijing, China, v. 4, p. 295–300, 2005.

TRUE FIRE. *7 guitars that changed music history*. 2016. <https://truefire.com/blog/sevens/7-guitars-that-changed-history/>. Last access:10/25/2019.

WAGNER, G. B. Análise modal operacional no domínio do tempo: Um estudo crítico dos métodos de identificação. Pontifícia Universidade Católica, Rio de Janeiro, Brazil, 2017.

WALLMARK, Z. et al. Embodied listening and timbre: Perceptual, acoustical, and neural correlates. *Music Percpetion*, Los Angeles, California, v. 35, n. 3, p. 332–363, 2018.

ZIEGLER, H. On the concept of elastic stability. *Eidgenössische Technische Hochschule*, Zürich, Switzerland, p. 351–403, 1956.

APPENDIX A – MATLAB routine - Guitar - Impacts on body

```
clc
clear all
close all

n_sensors = 4; % number of sensors
x = linspace(0,775,4);

%% Test 1

A_1 = xlsread('test_001_008.xlsx');

color = {[0.4 0.1 0.7]; [0.5 0.7 0.2]; [0 0.8 0.8]; [0.9 0.6 0]};
for i = 1:n_sensors % plot of time response – test 1
    y_1 = A_1(:,i);
%     figure
%     plot(y_1,'color',color{i});
%     %title(['Sensor s',num2str(i),' – Guitar – Body – Test 1']);
end

%% Test 2

A_2 = xlsread('test_001_009.xlsx');

for j = 1:n_sensors % plot of time response – test 2
    y_2 = A_2(:,j);
%     figure
%     plot(y_2,'color',color{j});
%     %title(['Sensor s',num2str(j),' – Guitar – Body – Test 2']);
end

```

```
31 %% Test 3
32
33 A_3 = xlsread('test_001_010.xlsx');
34
35 for j = 1:n_sensors % plot of time response - test 3
36     y_3 = A_3(:,j);
37 %     figure
38 %     plot(y_3,'color',color{j});
39 %     %title(['Sensor s',num2str(j),' - Guitar - Body - Test
       3']);
40 end
41
42 %% Average Responses
43
44 fs = 1e4;
45 T = 1/fs;
46 size_vib = 2e4;
47
48 bumps_1 = [3.295e3 3.494e4 6.414e4 9.296e4 1.216e5 1.515e5]; %
       bumps test 1
49 bumps_2 = [2.594e4 5.376e4 8.34e4 1.115e5 1.422e5 1.703e5]; %
       bumps test 2
50 bumps_3 = [2.506e4 5.174e4 8.19e4 1.098e5 1.391e5 1.686e5]; %
       bumps test 3
51 bumps = [bumps_1 bumps_2 bumps_3]; % vector of all bumps
52
53 % All tests
54 n_peaks = length(bumps);
55
56 for n = 1:n_peaks/3
57     for k = 1:n_sensors
58         A(:,k,n) = A_1(bumps_1(n):(bumps_1(n)+size_vib),k);
59     end
60 end
61
62 for n = 1:n_peaks/3
63     for k = 1:n_sensors
64         A(:,k,n+(n_peaks/3)) = A_2(bumps_2(n):(bumps_2(n)+
               size_vib),k);
```

```
65      end
66  end
67
68  for n = 1:n_peaks/3
69      for k = 1:n_sensors
70          A(:,k,n+(2*n_peaks/3)) = A_3(bumps_3(n):(bumps_3(n)+
                size_vib),k);
71      end
72  end
73
74  for i = 1:n_peaks
75      A(:,1,i) = A(:,1,i)-mean(A(:,1,i));
76      A(:,2,i) = A(:,2,i)-mean(A(:,2,i));
77      A(:,3,i) = A(:,3,i)-mean(A(:,3,i));
78      A(:,4,i) = A(:,4,i)-mean(A(:,4,i));
79      A(:,:,i) = A(:,:,i)/max(max(A(:,:,i)));
80  end
81
82  for n = 1:n_peaks
83      for k = 1:n_sensors
84          np = length(A);
85          freq = 0:(fs/np):(fs/2);
86          temp = abs(fft(A(:,k,n))/round(np/2));
87          Y(:,k,n) = temp(1:length(freq));
88      end
89  end
90
91  freq_s1 = squeeze(Y(:,1,:)); % sensor 1
92  freq_s2 = squeeze(Y(:,2,:)); % sensor 2
93  freq_s3 = squeeze(Y(:,3,:)); % sensor 3
94  freq_s4 = squeeze(Y(:,4,:)); % sensor 4
95
96  for k = 1:n_sensors
97      if k == 1
98          freq = freq(1:round(np/2));
99
100         figure
101         plot(freq,db(freq_s1),'k--','linewidth',0.3);
102         hold on
```

```
103         plot(freq,db(mean(freq_s1')),'linewidth',3,'color',
                color{k});
104         grid minor
105         xlabel('Frequency␣(Hz)','fontsize',12);
106         ylabel('Magnitude␣(db)␣','fontsize',12);
107         %title(['Average FFT - Guitar - Body - Sensor s',
                num2str(k)]);
108         xlim([20 320])
109
110     elseif k == 2
111         freq = freq(1:round(np/2));
112
113         figure
114         plot(freq,db(freq_s2),'k—','linewidth',0.3);
115         hold on
116         plot(freq,db(mean(freq_s2')),'linewidth',3,'color',
                color{k});
117         grid minor
118         xlabel('Frequency␣(Hz)','fontsize',12);
119         ylabel('Magnitude␣(db)','fontsize',12);
120         %title(['Average FFT - Guitar - Body - Sensor s',
                num2str(k)]);
121         xlim([20 320])
122
123     elseif k == 3
124         freq = freq(1:round(np/2));
125
126         figure
127         plot(freq,db(freq_s3),'k—','linewidth',0.3);
128         hold on
129         plot(freq,db(mean(freq_s3')),'linewidth',3,'color',
                color{k});
130         grid minor
131         xlabel('Frequency␣(Hz)','fontsize',12);
132         ylabel('Magnitude␣(db)','fontsize',12);
133         %title(['Average FFT - Guitar - Body - Sensor s',
                num2str(k)]);
134         xlim([20 320])
135
```

```
136     elseif k == 4
137         freq = freq(1:round(np/2));
138 
139         figure
140         plot(freq,db(freq_s4),'k—','linewidth',0.3);
141         hold on
142         plot(freq,db(mean(freq_s4')),'linewidth',3,'color',
                color{k});
143         grid minor
144         xlabel('Frequency␣(Hz)','fontsize',12);
145         ylabel('Magnitude␣','fontsize',12);
146         %title(['Average FFT - Guitar - Body - Sensor s',
                num2str(k)]);
147         xlim([20 320])
148     end
149 end
150 
151 figure
152 plot(freq,db(mean(freq_s1')),'color',color{1});
153 hold on
154 plot(freq,db(mean(freq_s2')),'color',color{2});
155 hold on
156 plot(freq,db(mean(freq_s3')),'color',color{3});
157 hold on
158 plot(freq,db(mean(freq_s4')),'color',color{4});
159 xlabel('Frequency␣(Hz)','fontsize',12);
160 ylabel('Spectral␣Density␣(g  /Hz)','fontsize',12);
161 %title('Superposition of average FFT''s - Guitar - Body - All
    sensors');
162 legend({'s1','s2','s3','s4'},'Location','best')
163 xlim([20 320])
164 
165 %% Output-only modal analysis
166 
167 B = [A_1; A_2];
168 [SV,F,Phi,I,SV_nums] = fdd(B,[],fs,[]); % frequency-domain
    decomposition
169 
170 figure
```

```
171 clf
172 for i = 1:size(Phi,2)
173     subplot(size(Phi,2),1,i)
174     z = Phi(:,i);
175     plot(x,abs(z).*cos(angle(z)))
176     hold on
177     plot(x,-abs(z).*cos(angle(z)))
178     hold off
179
180     if i == size(Phi,2)
181         xlabel('Structure position (mm)')
182     else
183         xticklabels([])
184     end
185     axis tight
186     ylabel(['Mode ' num2str(i)])
187 end
```